EUROfusion

Overview of Physics Studies on ASDEX Upgrade

The ASDEX Upgrade Programme is jointly run by IPP and EUROfusion

Hendrik Meyer
for the AUG and EUROfusion MST1 Teams

CCFE CULHAM CENTRE FOR FUSION ENERGY

ASDEX Upgrade

IPP

This work has been carried out within the framework of the EUROfusion Consortium and has received funding from the Euratom research and training programme 2014-2018 under grant agreement No 633053. The views and opinions expressed herein do not necessarily reflect those of the European Commission.

AUG programme – To prepare ITER and DEMO

High heating power

P_{NBI}= 20 MW

P_{ECRH}= 8 MW

P_{ICRF}= 7MW

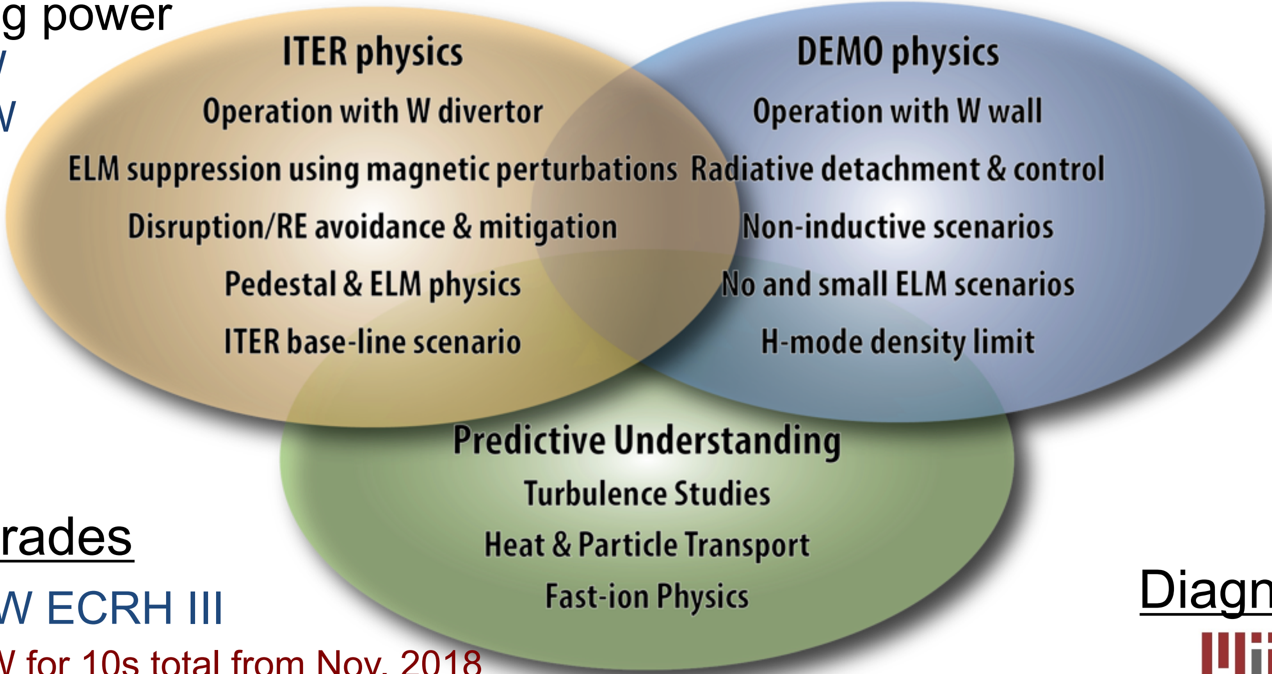

Medium size

R_0 = 1.65 m

a = 0.5 m

κ = 1.8

δ = 0.4

V_{pl} = 13 m^3

B_t = 3.2T

I_p = 1.4 MA

Plant upgrades

- 2 (4) MW ECRH III
  - 8 MW for 10s total from Nov. 2018
- 16 fast power supplies for internal coils
  - ELM control, MHD, scenarios
- Boron dropper — R. Lunsford FIP/2-3 (Thu 15:00) — PPPL

Diagnostic upgrades

- MIT Correlation ECE
- LPP Correlation Doppler Reflectometer
- Fast Edge Charge Exchange
- Fast Helium Beam Spectroscopy

From the outside to the core

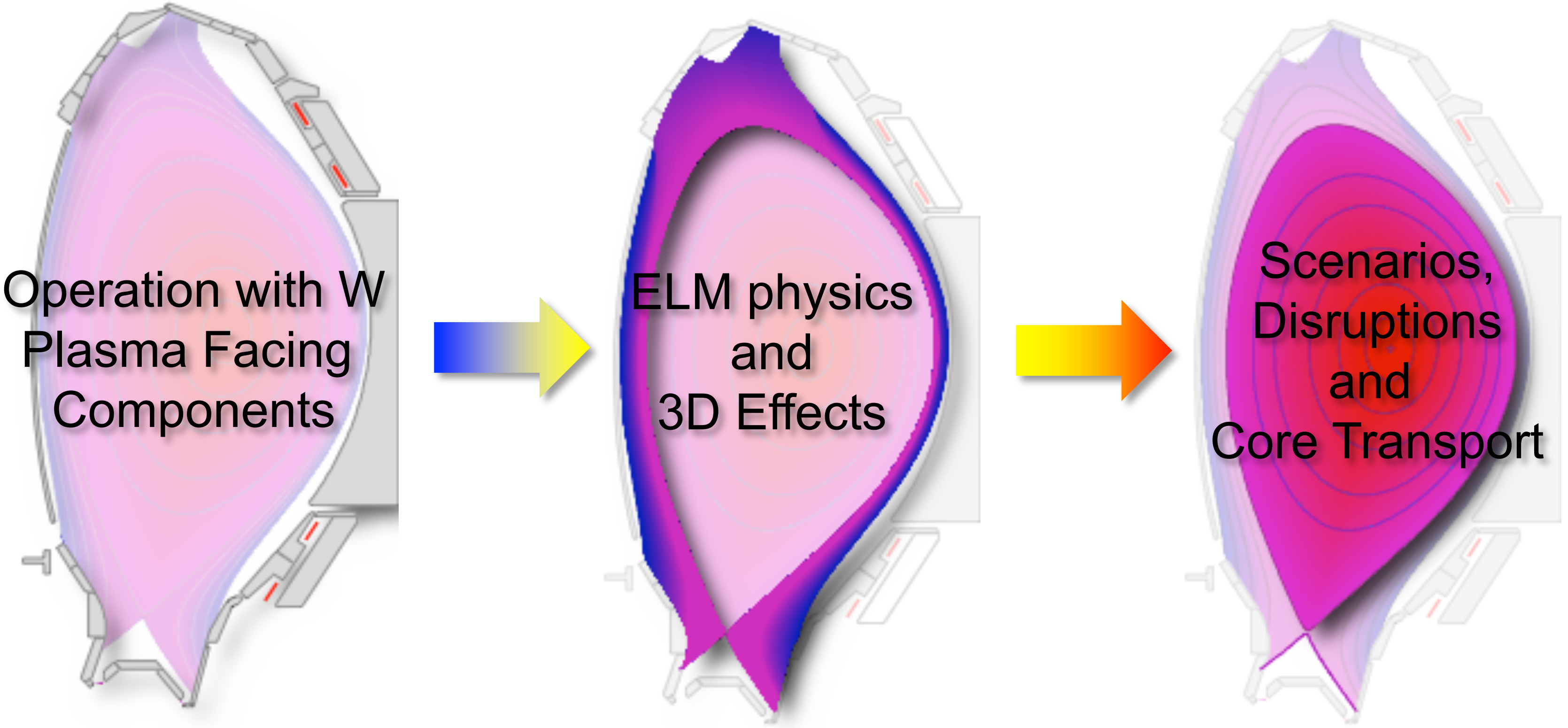

From the outside to the core

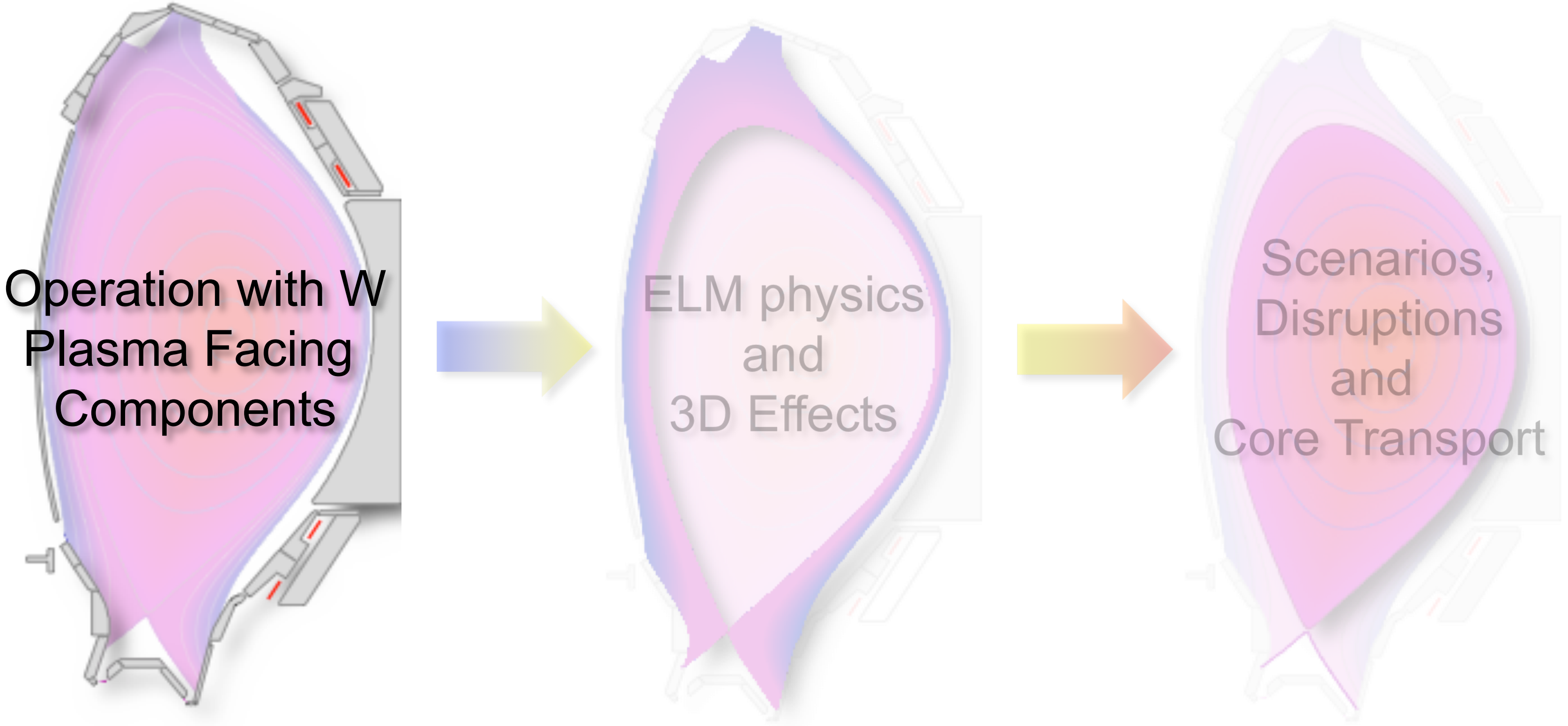

Edge-ICRF interaction – W melt motion

Improved understanding of the edge ICRF interaction

J.M. Noterdaeme
EX/P8-23 (Fri 14:00)

- Operation of ICRF with a W wall requires understanding of the edge interaction: *Avoid W sputtering, improve coupling*

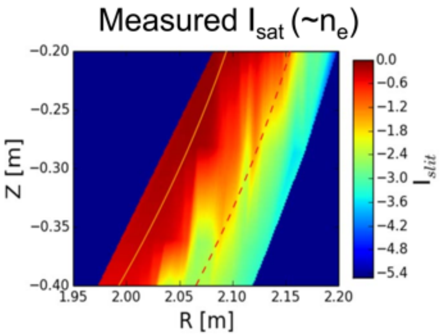

ZHANG, W. et al., Nuclear Fusion 57 (2017) 116048

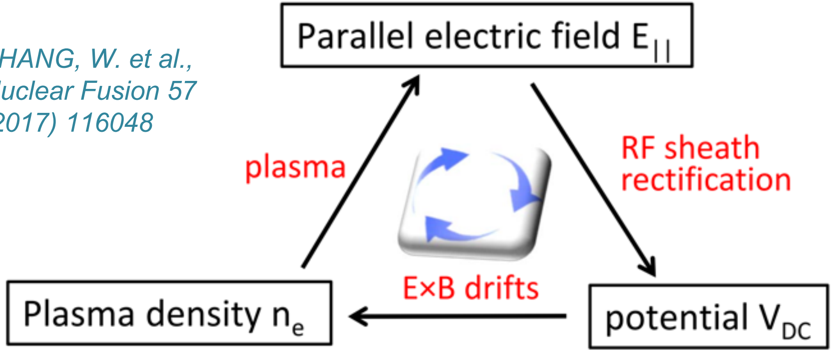

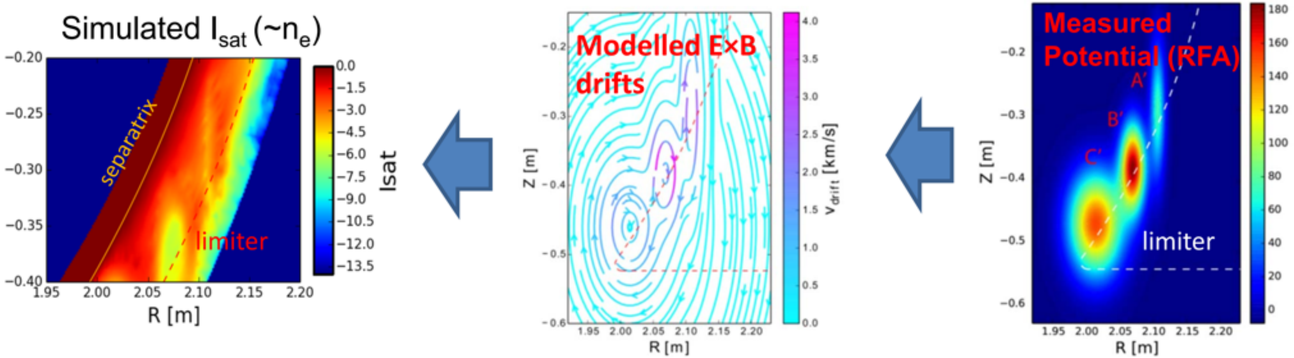

- Self-consistently coupled codes
  - RF E-field (RAPLICASOL)
  - Sheath-rectified (DC) field (SSWICH)
  - Induced E×B convection (EMC3-EIRENE)
- Convective cells well modelled, in good agreement with measurements

New 3-strap antenna avoids the issue

Improved understanding of the edge ICRF interaction

- Operation of ICRF with a W wall requires understanding of the edge interaction: *Avoid W sputtering, improve coupling*

J.M. Noterdaeme
EX/P8-23 (Fri 14:00)

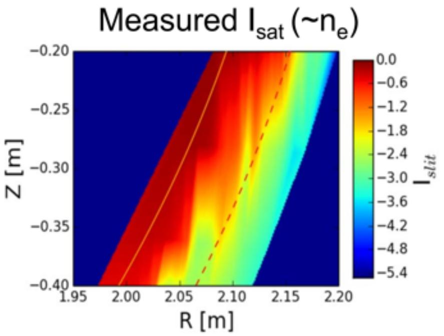

ZHANG, W. et al., Nuclear Fusion 57 (2017) 116048

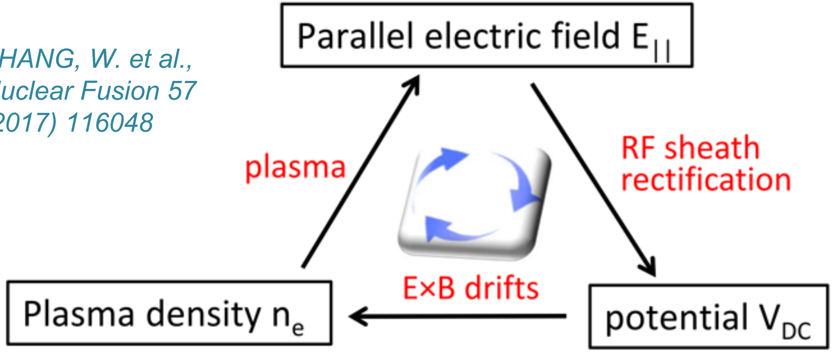

- Self-consistently coupled codes
  - RF E-field (RAPLICASOL)
  - Sheath-rectified (DC) field (SSWICH)
  - Induced E×B convection (EMC3-EIRENE)

- Convective cells well modelled, in good

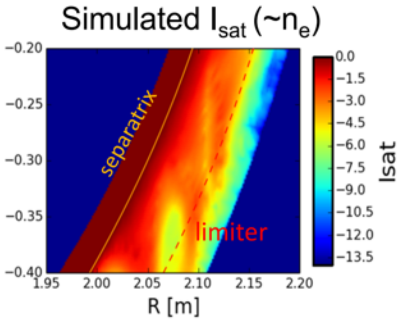

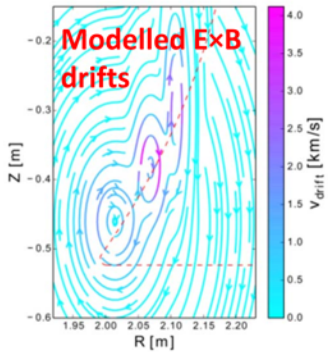

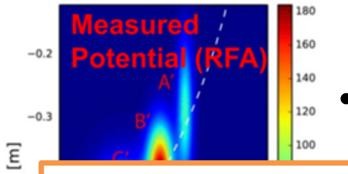

Three-ion (H-^{3}He-D) ICRF ITER H plasma relevant heating scenario demonstrated

Y. Kazakov EX/8-1 (Fri 15:20)

JET, C-Mod: *KAZAKOV, Y. O. et al., Nature Physics 13 (2017) 973.*

New 3-strap antenna avoids the issue

Modelling of Melt-motion in good agreement with experiment

- First observation of melt motion due to ELM transient.
  - Exposure of misaligned targets on divertor manipulator.
- Simultaneous measurement of T_{surf} and I_{emiss}.
  - During ELMs significant non-thermal current fraction.

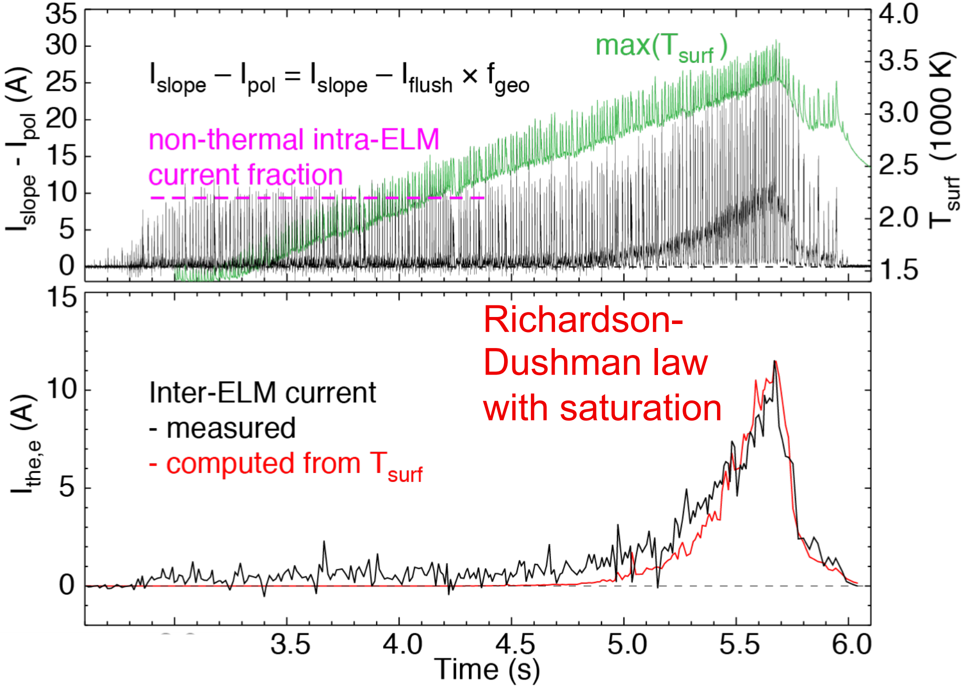

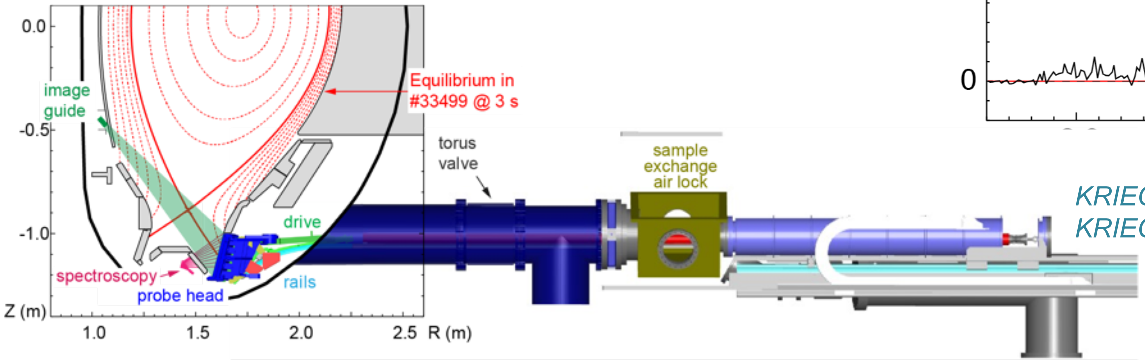

KRIEGER, K. et al., Physica Scripta 2017 (2017) 014030
KRIEGER, K. et al., 23rd PSI, 17-22 June 2018, Princeton, USA

Modelling of Melt-motion in good agreement with experiment

- First observation of melt motion due to ELM transient.
  - Exposure of misaligned targets on divertor manipulator.
- Simultaneous measurement of T_{surf} and I_{emiss}.
  - During ELMs significant non-thermal current fraction.
- MEMOS 3D simulations of surface deformation and melt displacement agree with experiment.
  - Dominant force: $j \times B$

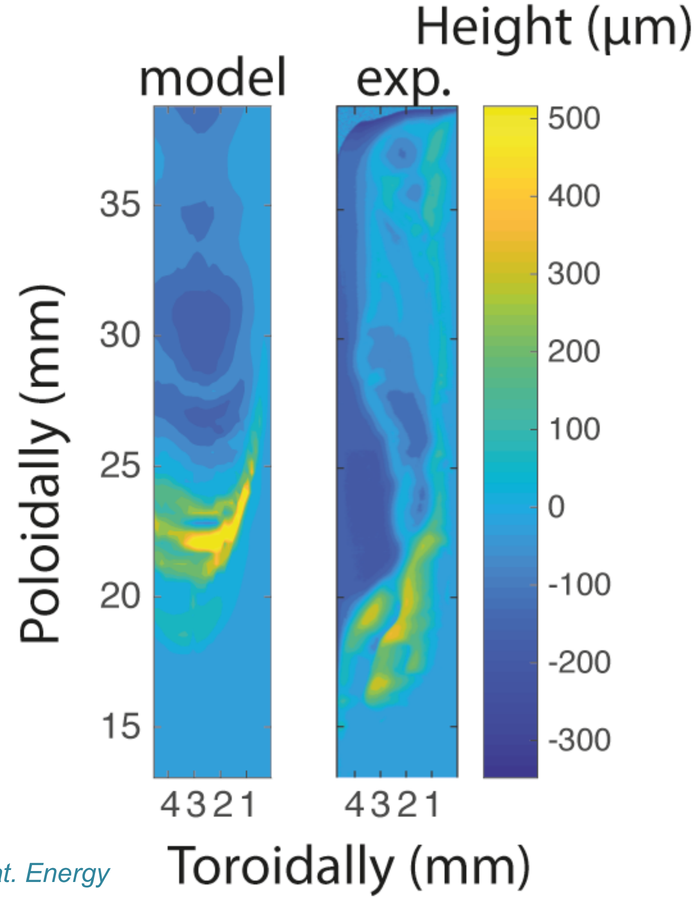

THORÉN, E. et al., submitted to Nucl. Mat. Energy

From the outside to the core

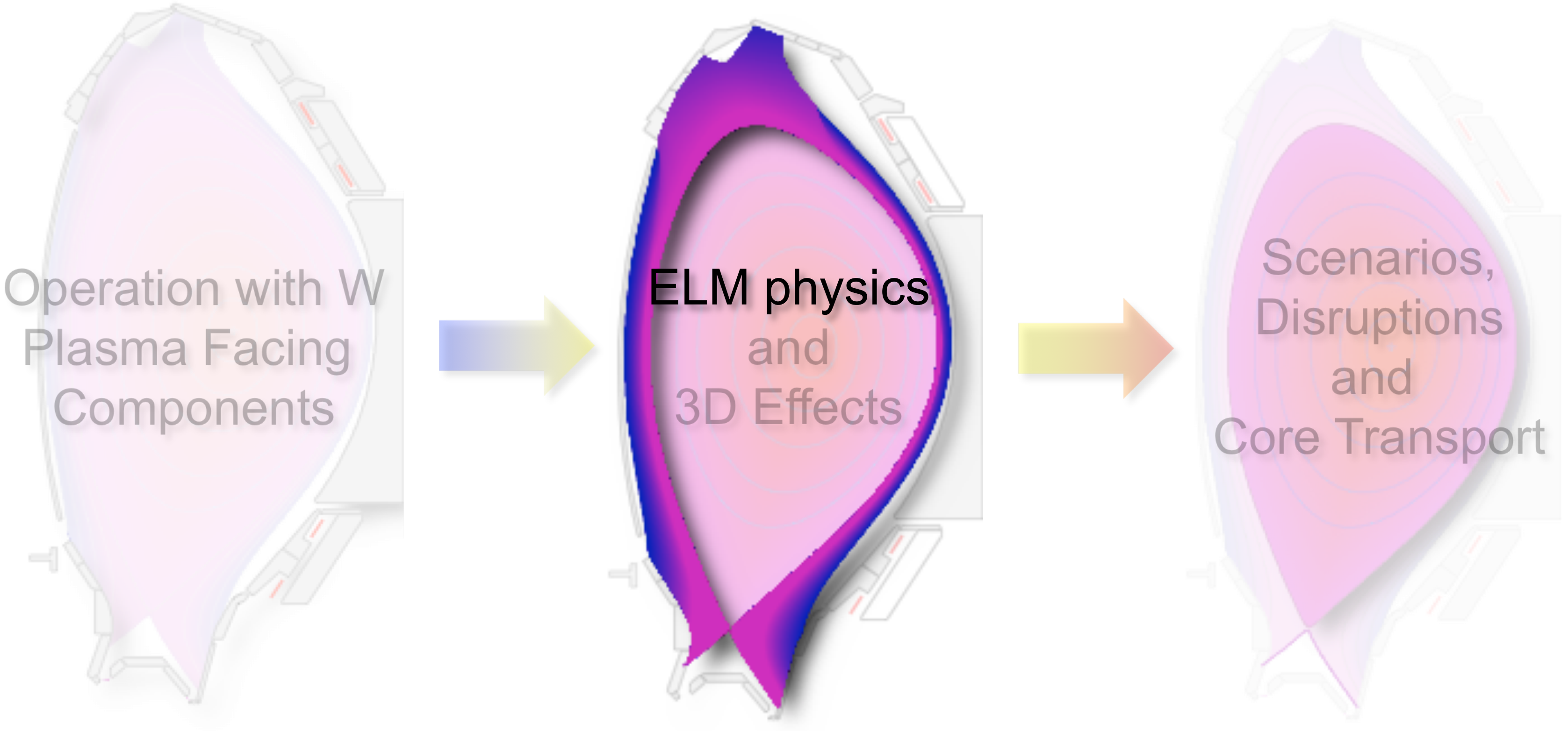

ELM crash modelling – beam ion acceleration during ELM – ELM cycle

Non-linear resistive MHD reproduces experimental details of ELM crash

Measurement

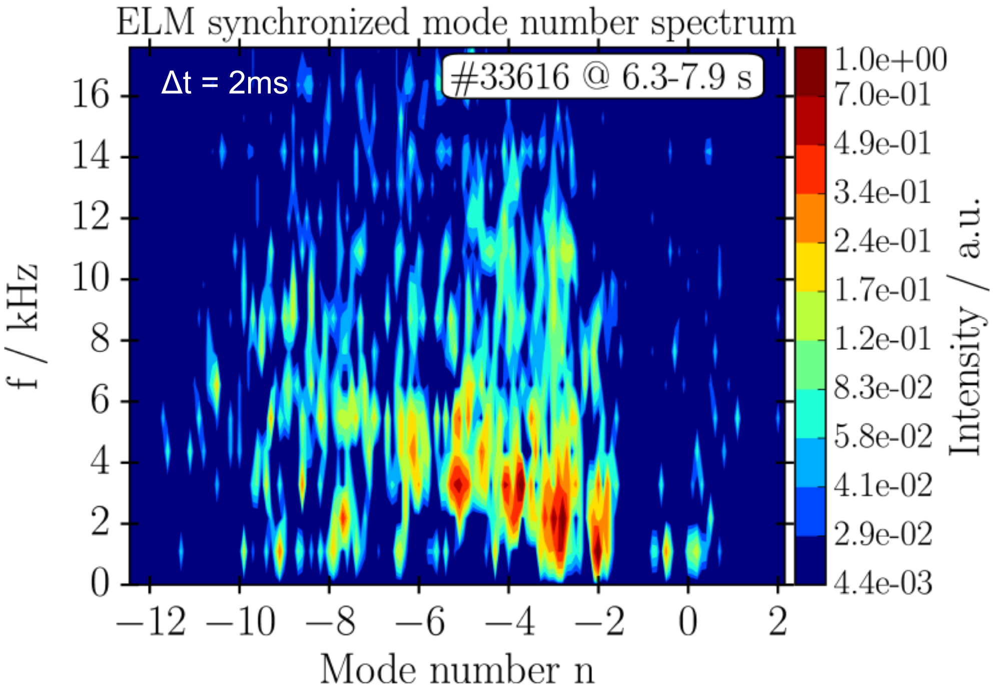

- New analysis technique ⟹ mode spectrum during the ELM crash.

MINK, A. et al., Nuclear Fusion 58 (2018) 026011.

Non-linear resistive MHD reproduces experimental details of ELM crash

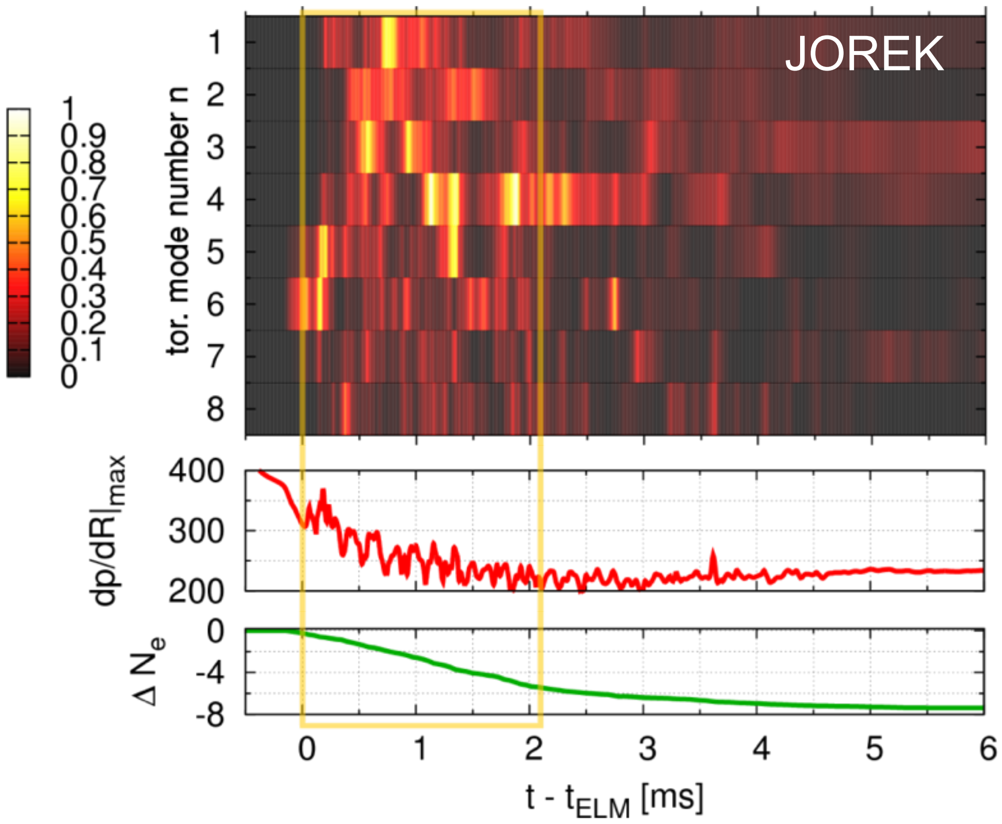

S.J.P. Pamela OV/4-4 (Tue 15:25)

- New analysis technique ⟹ mode spectrum during the ELM crash.
- JOREK reproduces
  - Mode numbers
  - Gradients and particle losses
  - Here: Growth rates agree.
- n=1 is important for mode coupling.

JOREK: Reduced non-linear resistive MHD

Parallel E-field from reconnection during the ELM accelerates beam ions

J. Galdon-Quiroga EX/P8-26 (Fri 14:00)

- Population of lost fast-ions measured with $E_{FI} \gg E_{inj}$.
  - Correlated with NBI sources and ELMs.

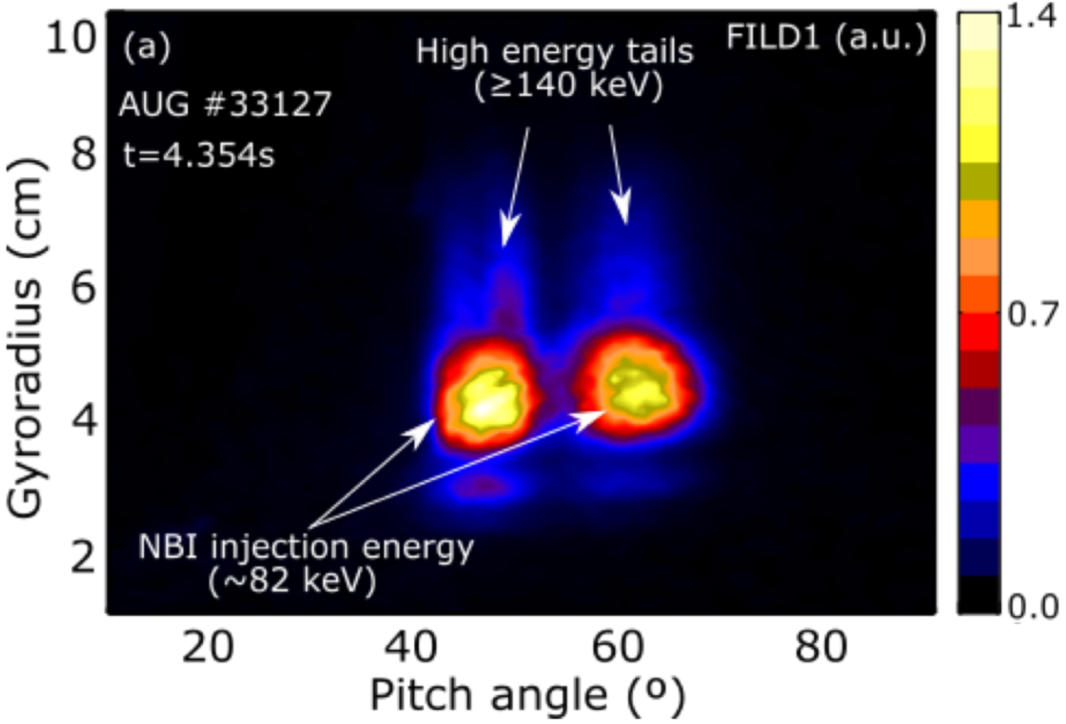

GALDON-QUIROGA, J. et al., Phys. Rev. Lett. 121 (2018) 025002.

Parallel E-field from reconnection during the ELM accelerates beam ions

J. Galdon-Quiroga EX/P8-26 (Fri 14:00)

- Population of lost fast-ions measured with $E_{FI} \gg E_{inj}$.
  - Correlated with NBI sources and ELMs.
- Well localised velocity-space structures.
  - From inversion of FILD data.

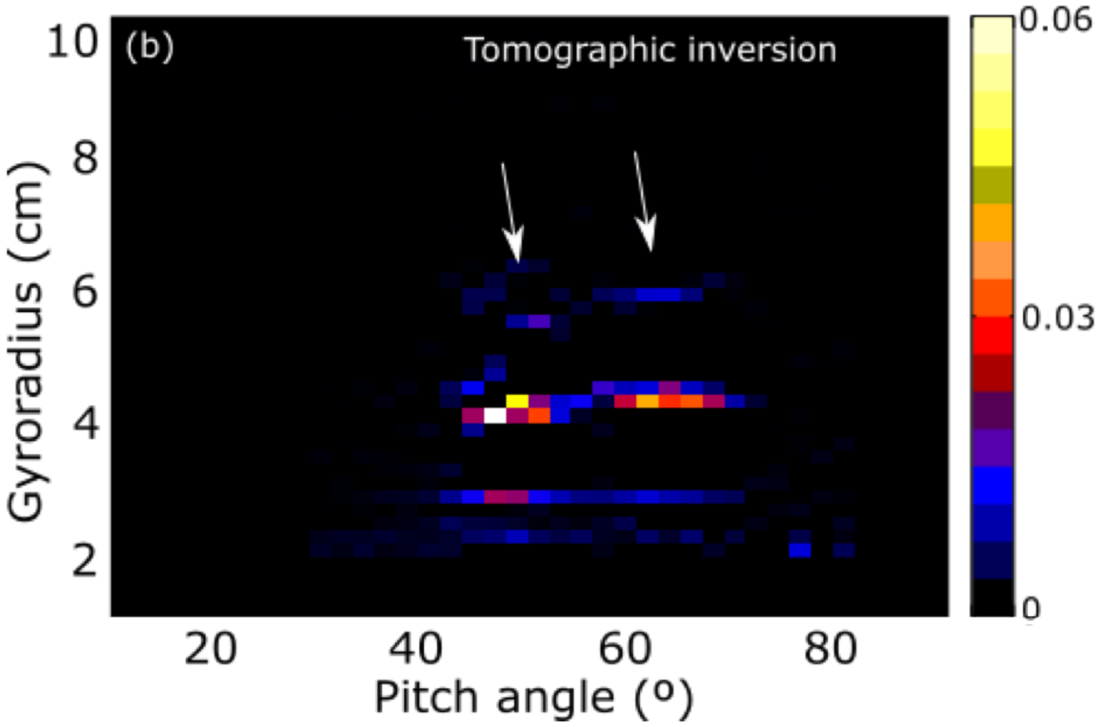

GALDON-QUIROGA, J. et al., Phys. Rev. Lett. 121 (2018) 025002.

Edge radial E-field dominated by $\nabla p/n$ during most of the ELM cycle

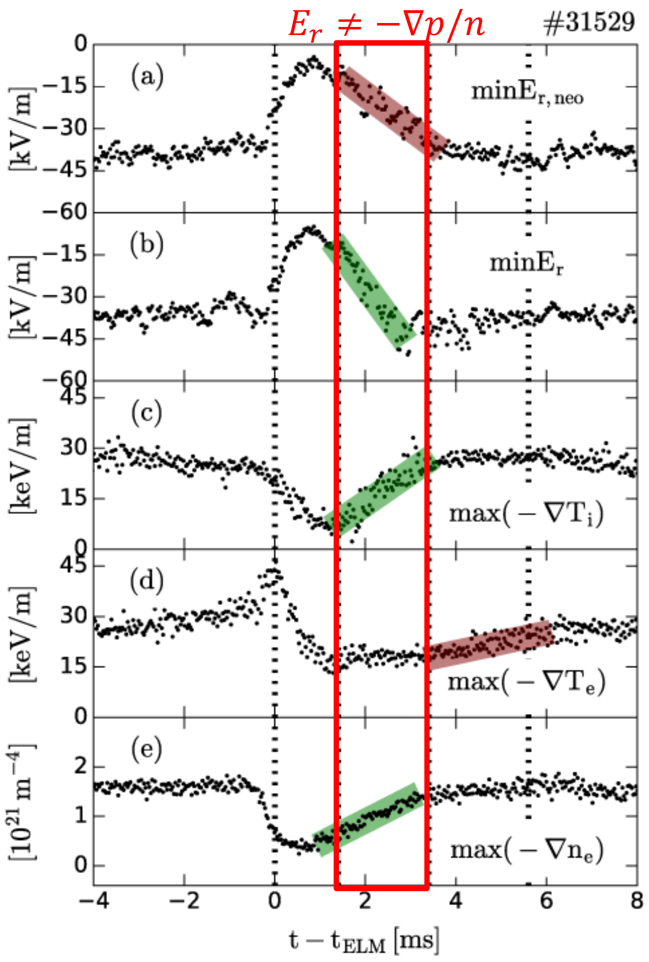

- New fast edge charge exchange system.
  $\Longrightarrow$ **E_r and T_i at $\Delta t = 200\ \mu s$**
  - All kinetic profiles measurable on a fast time scale.

- E_r evolves on similar time scale as n_e and T_i, T_e evolves slower

- Different phases coincide with edge mode activity.

CAVEDON, M. et al., Plasma Physics and Controlled Fusion 59 (2017) 105007

Edge radial E-field dominated by $\nabla p/n$ during most of the ELM cycle

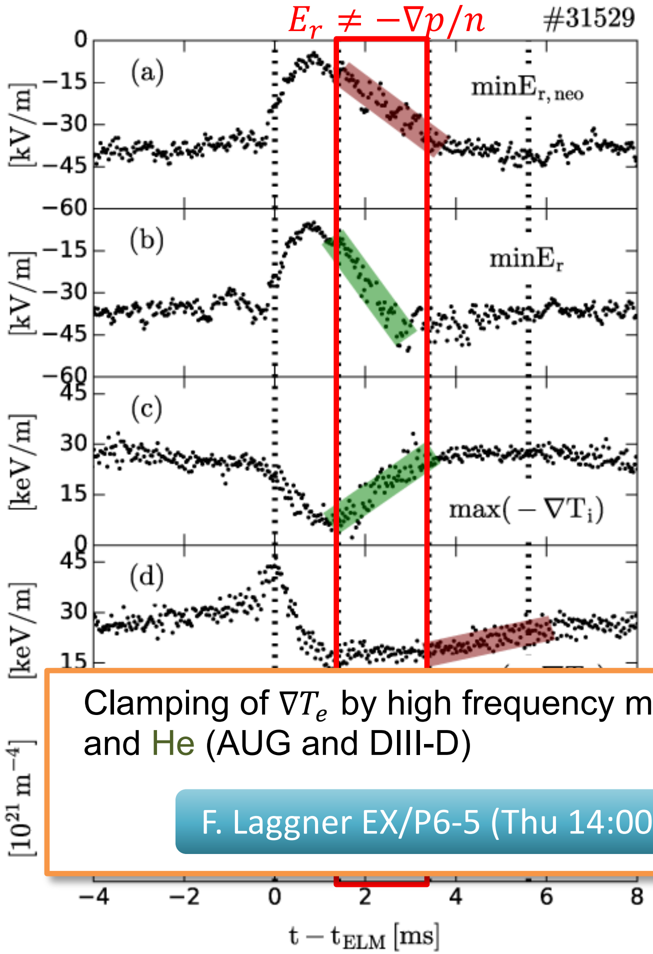

- New fast edge charge exchange system.
  $\Longrightarrow$ $\boldsymbol{E_r}$ **and** $\boldsymbol{T_i}$ **at** $\boldsymbol{\Delta t = 200\ \mu s}$
  - All kinetic profiles measurable on a fast time scale.

- E_r evolves on similar time scale as n_e and T_i, T_e evolves slower

nt p … y.

Clamping of ∇T_e by high frequency mode in D, H and He (AUG and DIII-D)

F. Laggner EX/P6-5 (Thu 14:00)

Edge Ion heat transport studies in D and He (ASTRA)

E. Viezzer EX/P8-5 (Fri 14:00)

CAVEDON, M. et al., Plasma Physics and Controlled Fusion 59 (2017) 105007

From the outside to the core

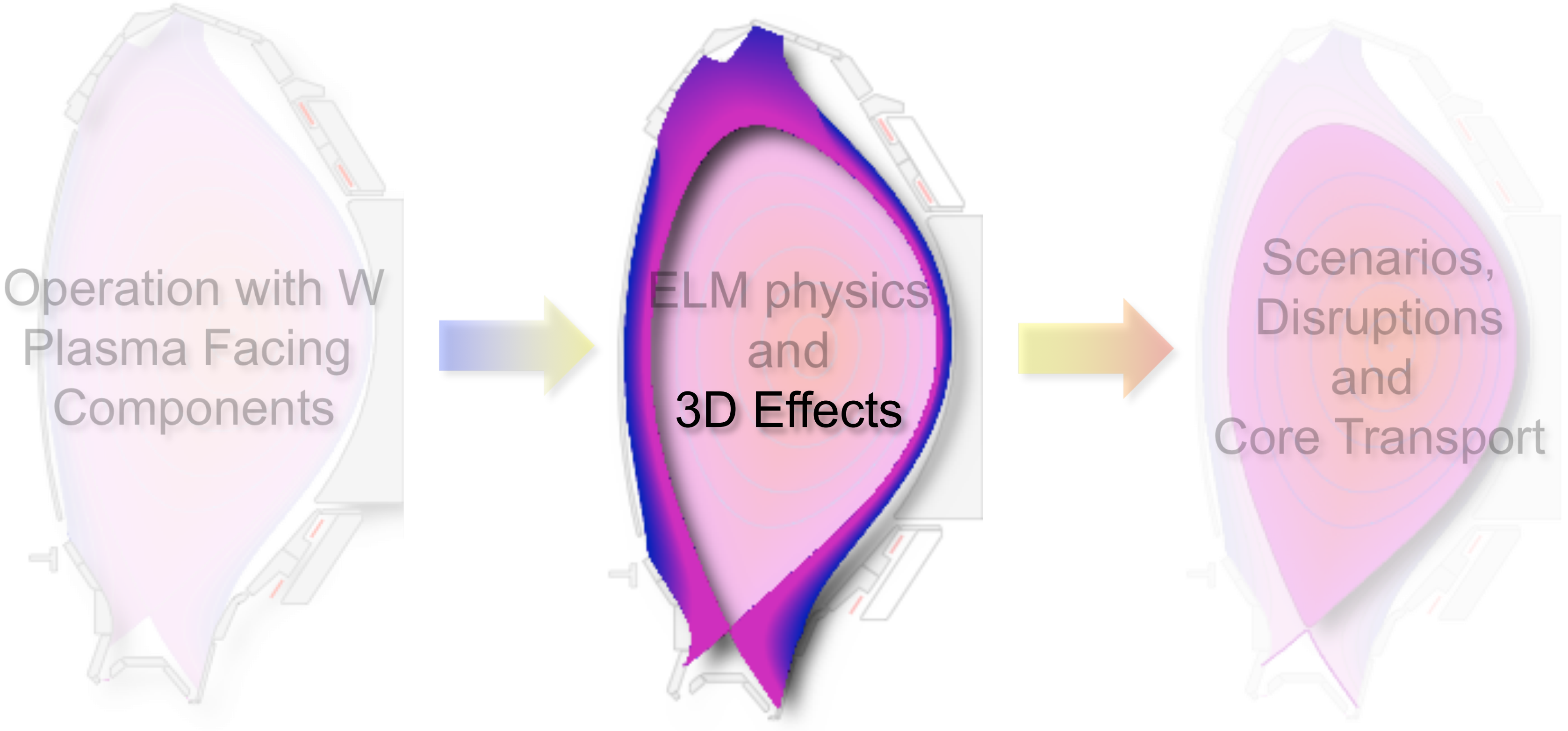

ELM suppression – Localised ballooning mode –SOL profiles

ELM suppression with $\omega_{e,\perp} \neq 0$ – no rotation threshold

Hypothesis:

- Island forms at the pedestal top $\Rightarrow$ pedestal below PB stability limit.
- Tearing requires $\omega_{e,\perp} \approx 0$ at rational q.
- Supported by JOREK modelling.

Experiment:

- No rotation threshold found.
- ELM suppression with finite $\omega_{e,\perp}$.
- No experimental evidence of island.

Possible Solution:

- ELM suppression through resistive response **if** kinetic effects destroy shielding of perturbation.

SUTTROP, W. et al., Nuclear Fusion 58 (2018) 096031

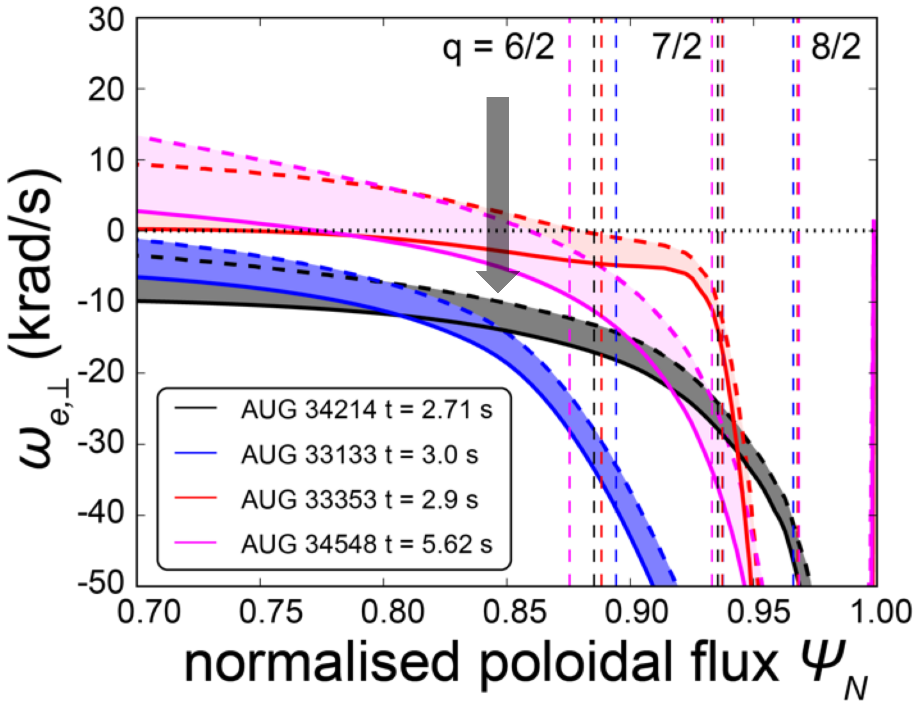

W. Suttrop EX/7-3 (Fri 9:10)

Helical localised Ballooning Mode destabilised by 3D perturbation

- Direct evidence for altered edge stability due to magnetic perturbations (MP).
- Mode observed in particular time during static rotation of MP field.
    - Localised on particular field line.
- No tearing signature, no phase delay between n_e and T_e $\Longrightarrow$ ideal mode.
- Ideal ballooning theory $\Longrightarrow$ mode grows on least stable field line.

COTE, T. B. et al., Submitted to Nucl. Fusion, 2018.

WILLENSDORFER, M. et al., Phys. Rev. Lett. 119 (2017) 085002.

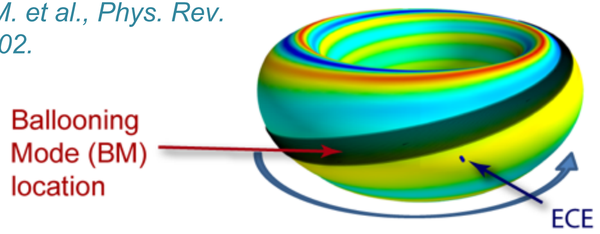

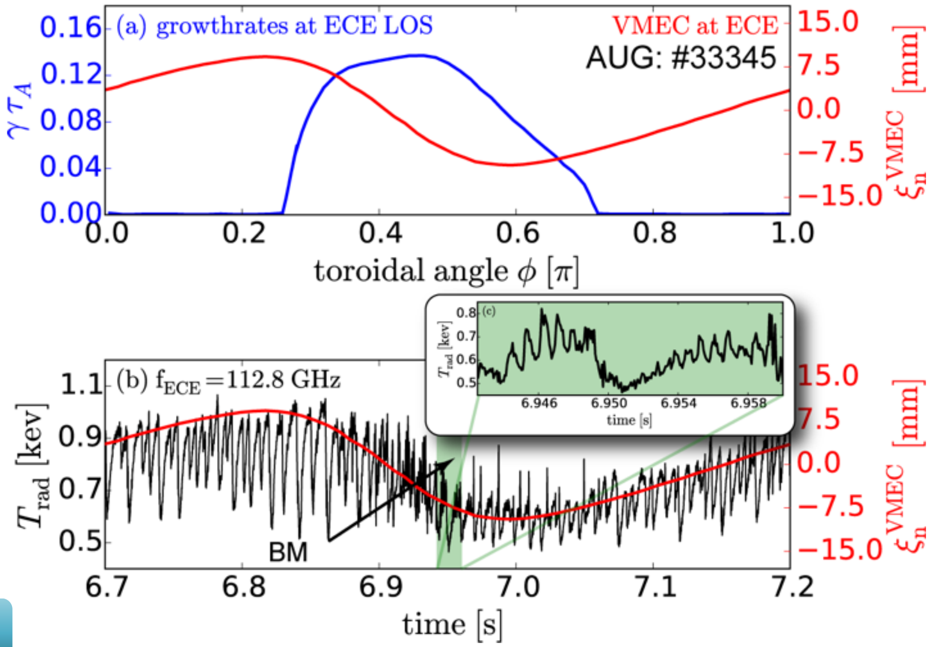

M. Willensdorfer EX/P8-20 (Fri 14:00)

2D target footprint from 3D magnetic perturbations vanishes approaching detachment

L-mode

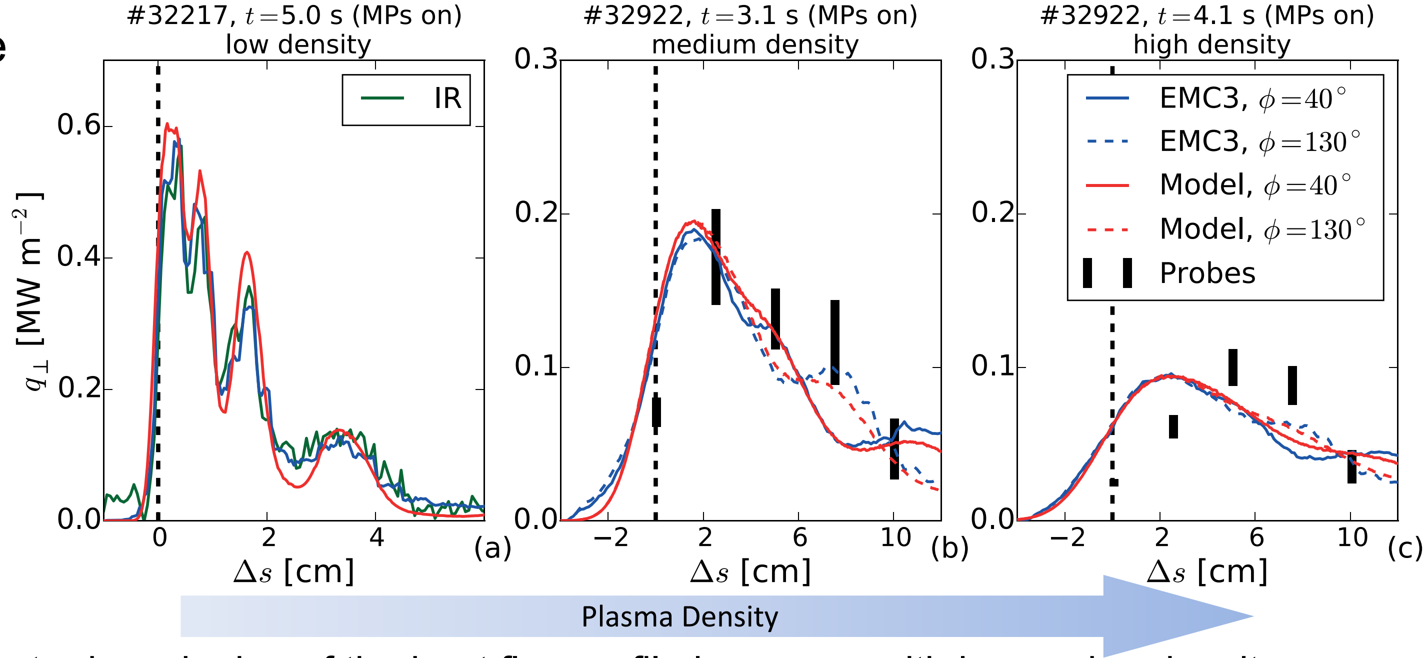

- Divertor broadening of the heat flux profile increases with increasing density.
- 2D spiral pattern is "washed" out.
- Good agreement between EMC3-EIRENE modelling and measurements for attached profiles.

FAITSCH, M. et al., Plasma Physics and Controlled Fusion 59 (2017) 095006.

BRIDA, D. et al., Nuclear Fusion 57 (2017) 116006.

From the outside to the core

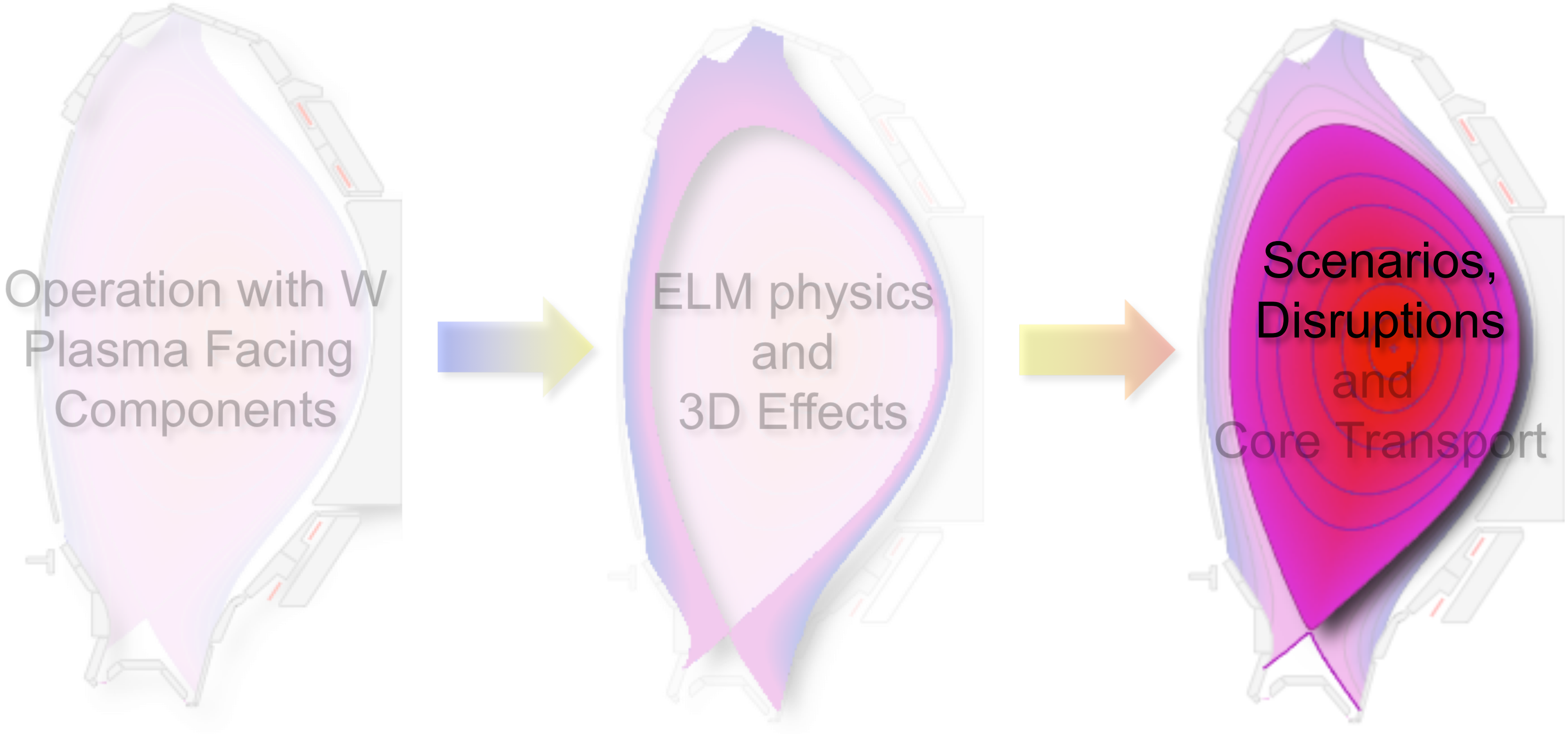

No and Small ELMs – H-mode density limit – Runaway electrons

Heat loads in I-mode have been characterised

- I-mode operating space has been extended to higher Greenwald fraction.
  - Stationary: $\bar{n}/n_{GW} = 0.58$
  - Transient: $\bar{n}/n_{GW} = 0.7$
- β_{pol} feedback allows access to stationary I-modes at $H_{H98(y,2)} = 0.8$ and $\bar{n}/n_{GW} = 0.58$.
- Stationary power fall of length of I-mode are in between L-mode and H-mode.
  - Intermittent density bursts could lead to high heat loads in the divertor.

T. Happel EX/2-3 (Wed 11:25)

HAPPEL, T. et.al. PSI 2018

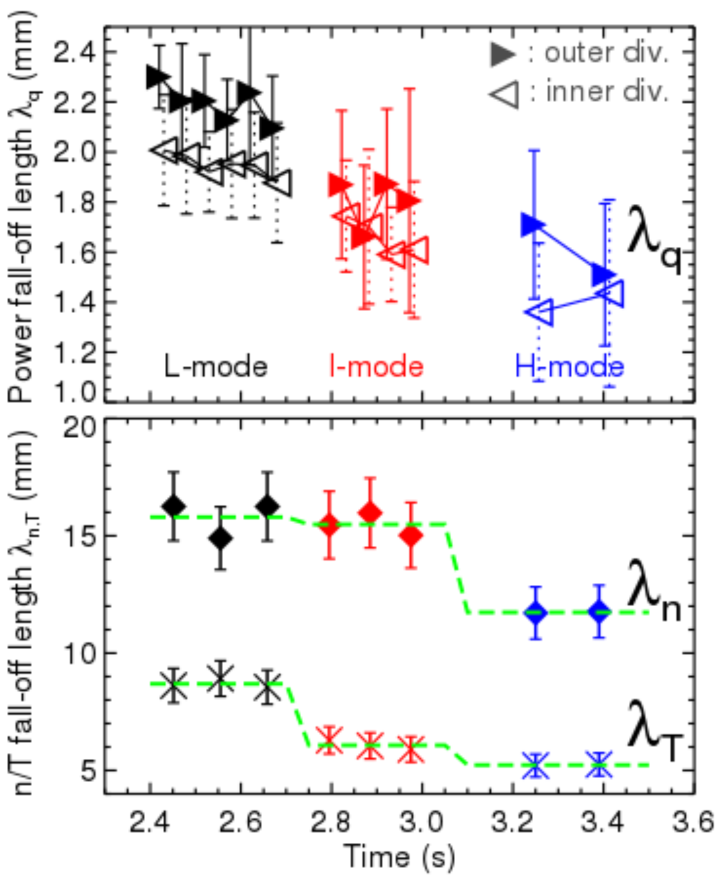

Increased ballooning transport at separatrix ⟹ small ELMs

B. Labit EX/2-5 (Wed 12:05)

HARRER, G. F. et al., Nuclear Fusion (2018)

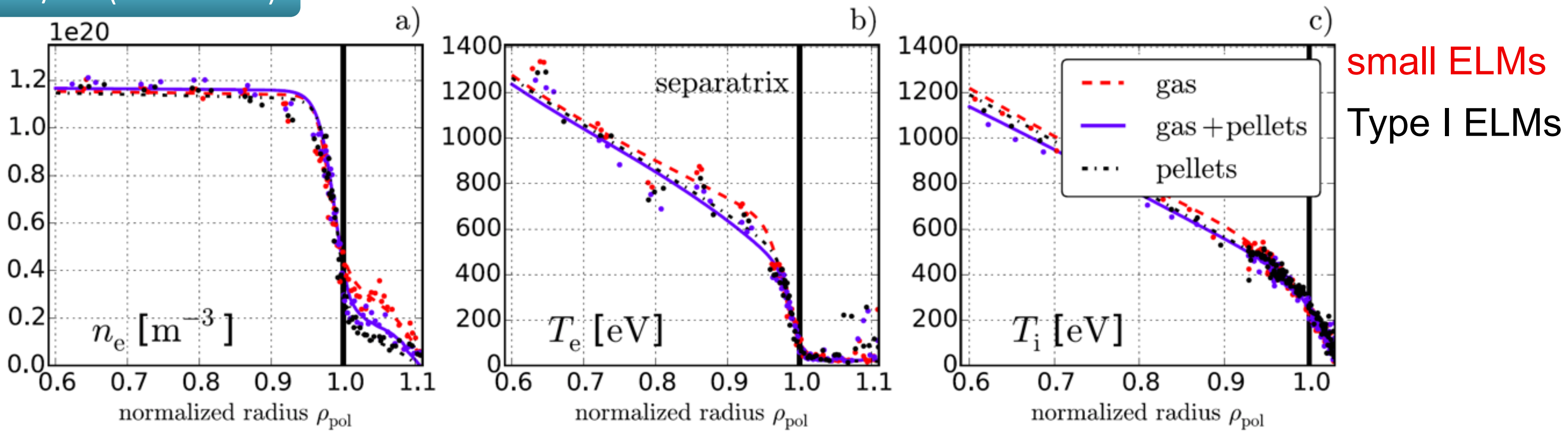

- Observed changes of small ELM behaviour are consistent with drift-ballooning stability.
  - Small ELMs become stronger at higher n_{sep} and lower q'/q.
- Transport at separatrix reduces pedestal width ⟹ ***no type-I ELMs***
- Scenario is close to high density ($\bar{n}/n_{GW} = 0.85$) ITER base-line scenario.

Increased ballooning transport at separatrix ⟹ small ELMs

B. Labit EX/2-5 (Wed 12:05)

HARRER, G. F. et al., Nuclear Fusion (2018)

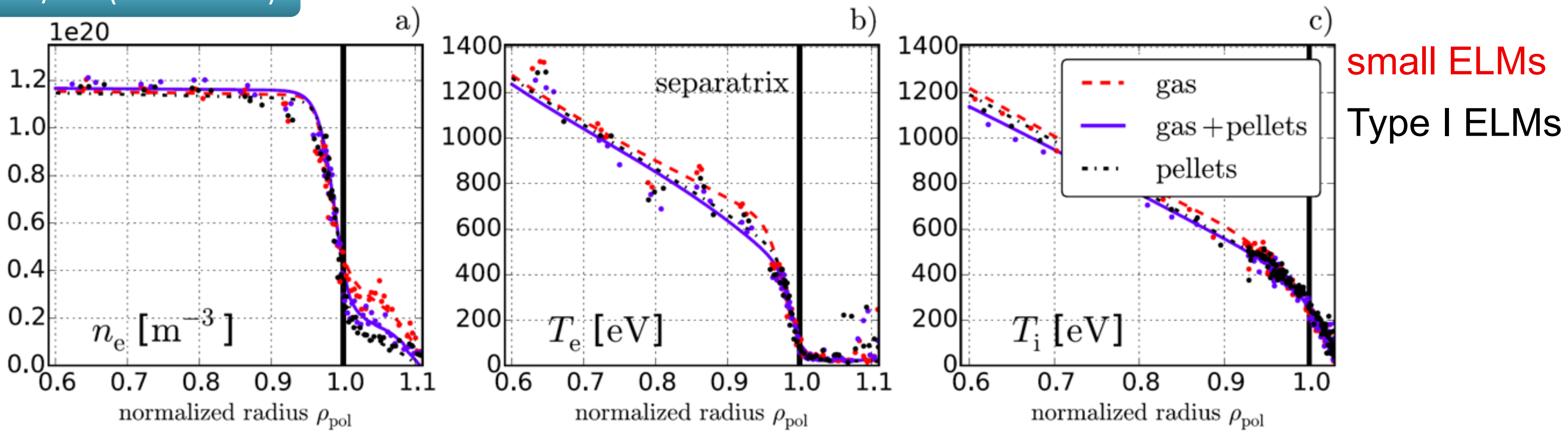

• C … ur a … .

and

• T … widt

• S … = 0.

High n_{sep} also affects type-I ELM stability
Shift of $n_e^{pos} \Longrightarrow$ shift of $p(r) \Longrightarrow$ reduced p_{ped}
Reduction of ITER confinement 30%-40%

M. Dunne EX/P8-2 (Fri 14:00) AUG, CMOD

L. Frassinetti EX/P8-22 (Fri 14:00) AUG, TCV, JET

Detailed studies of ITER baseline scenario:

- New low $\nu^\star \sim (2-3)\nu^\star_{ITER}$ using MP density pump-out.
- MHD stable at high density and low rotation.

T. Pütterich EX/P8-4 (Fri 14:00)

Ballooning limit at pedestal foot consistent with H-mode density limit

- Measured Ballooning parameter

$$\alpha_{sep} = \frac{Rq_{cyl}^2}{B_{tor}^2/2\mu_0} \cdot \frac{p_{sep}}{\langle\lambda_p\rangle}$$

  saturates at $\alpha_{crit} \approx 2.5$.
  - Data from edge Thomson Scattering.
- Limit to separatrix density.

Conjecture:

- Increased turbulent transport leads to H-mode density limit (HDL).

$\langle\lambda_p\rangle$: poloidially averaged pressure decay length a separatrix

EICH, T. et al., Nuclear Fusion 58 (2018) 034001.

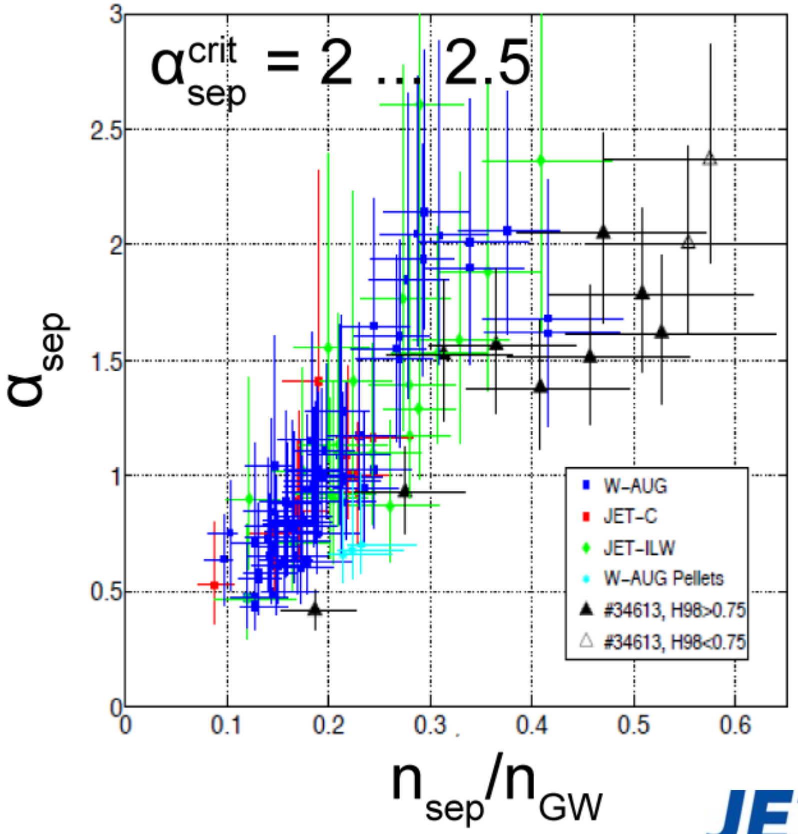

Runaway Electron beam dissipation by mass injection agrees with modelling

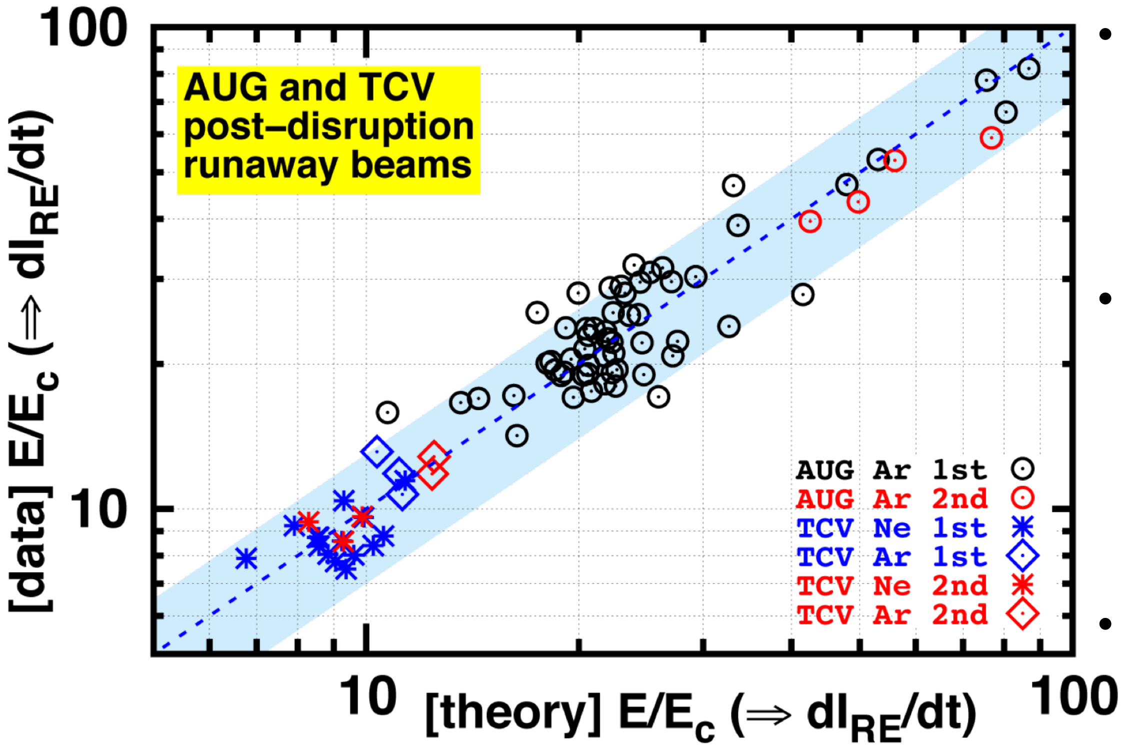

- Fast electron energy dissipated by Coulomb collisions.
  - Quantum mechanical processes need to be considered.
- Good agreement between data and theory on a statistical level.
  - Effective critical field from Fokker Planck solver.

    HESSLOW, L. et al., Phys. Rev. Lett. 118 (2017) 255001.
- Confidence in predicting mass needed for ITER RE mitigation with 2nd injection.

G. Papp et.al. 15th IAEA TM EP, Princeton, NJ, USA

Runaway Electron beam dissipation by mass injection agrees with modelling

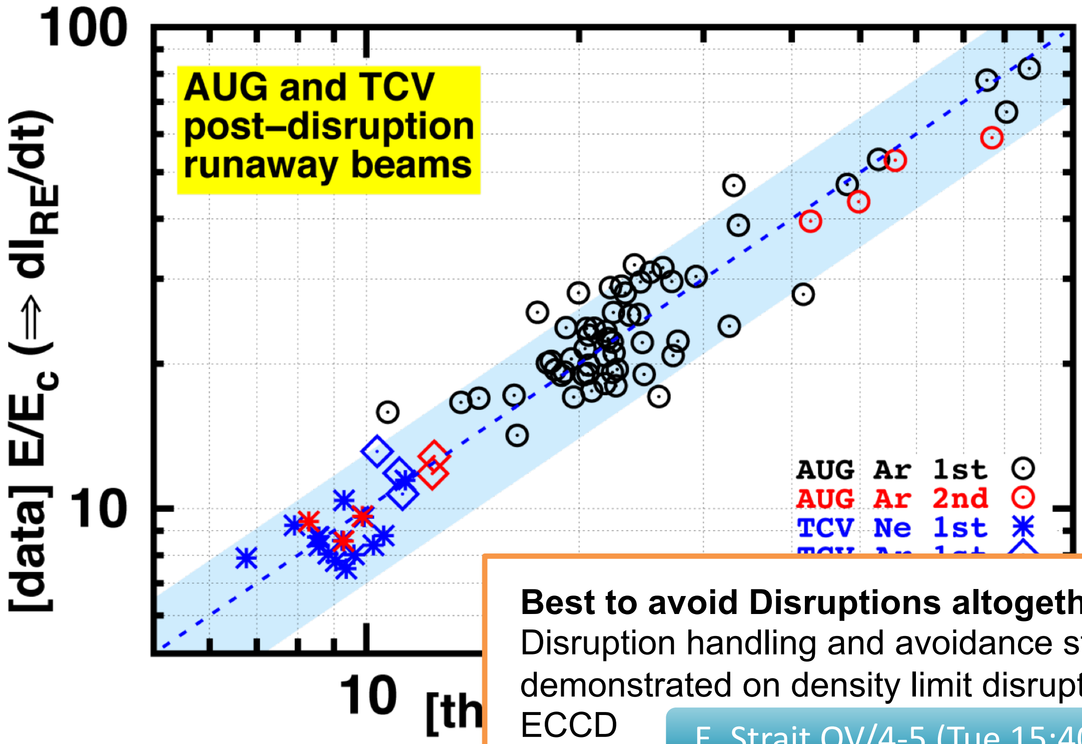

- Fast electron energy dissipated by Coulomb collisions.
  - Quantum mechanical processes need to be considered.
- Good agreement between data and theory on a statistical level.
  - Effective critical field from Fokker Planck solver.

HESSLOW, L. et al., Phys. Rev. Lett. 118 (2017) 255001.

- …ence in predicting mass … for ITER RE mitigation … injection.

Best to avoid Disruptions altogether
Disruption handling and avoidance strategy demonstrated on density limit disruptions using ECCD

E. Strait OV/4-5 (Tue 15:40)

G. Papp et.al. 15th IAEA TM EP, Princeton, NJ, USA

From the outside to the core

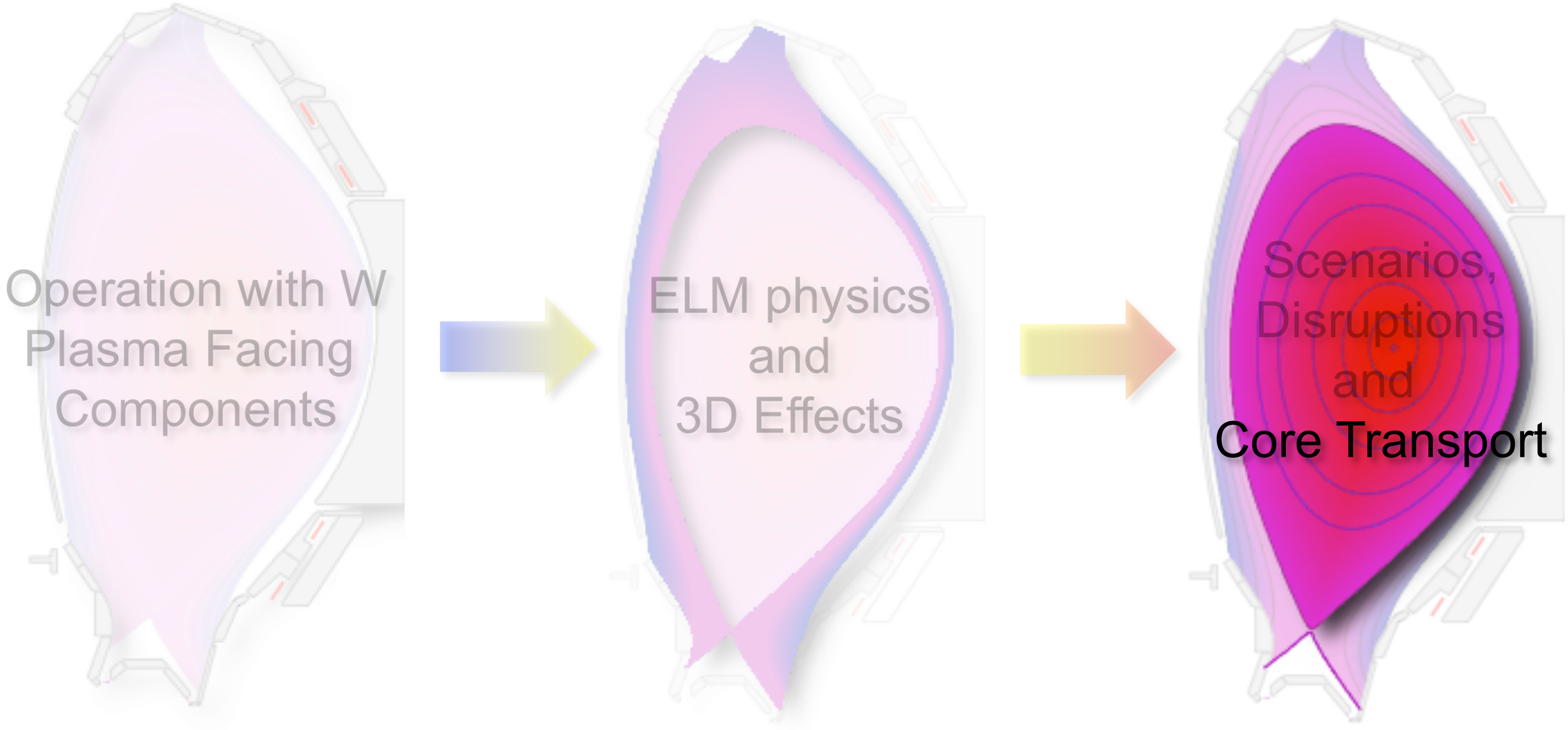

Isotope Effect – Density Eddy Tilt Angle – Comparison with Gyro-kinetics

Lower Confinement in H Explained by Larger Ion Heat Flux

SCHNEIDER, P. et al., Nuclear Fusion 57 (2017) 066003.

<u>*Experiment:*</u>

- Profile matched D and H L-mode discharges.
  - Dominant e⁻-heating ($P^D_{net} = 1.06\ MW$, $P^H_{net} = 1.39\ MW$).

<u>*Simulation:*</u> (ASTRA)

- Critical gradient model for χ_e and χ_i without mass dependence *[Garbet PPCF 2004].*
  - Model adjusted to fit D and then applied to H.
- Only collisional energy exchange is mass dependent.

$$P_{ie} \propto \frac{m_e}{m_i}\frac{n^2}{T_e^{3/2}}(T_e - T_i) \Longrightarrow P^H_{ei} = 2P^D_{ei}$$

- Profiles and confinement degradation reproduced.

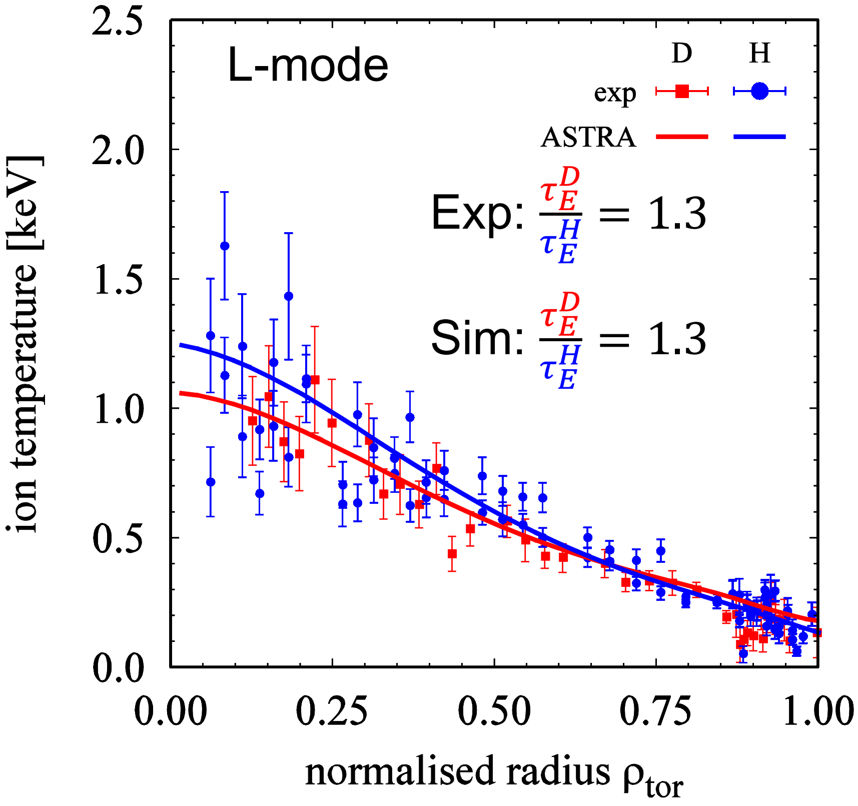

Lower Confinement in H Explained by Larger Ion Heat Flux

SCHNEIDER, P. et al., Nuclear Fusion 57 (2017) 066003.

<u>*Experiment:*</u>

- Profile matched D and H L-mode discharges.
  - Dominant e⁻-heating ($P^D_{net} = 1.06\ MW$, $P^H_{net} = 1.39\ MW$).

<u>*Simulation:*</u> (ASTRA)

- Critical gradient model for χ_e and χ_i without mass dependence *[Garbet PPCF 2004].*
  - Model adjusted to fit D and then applied to H.
- Only collisional energy exchange is mass dependent.

$$P_{ie} \propto \frac{m_e}{m_i}\frac{n^2}{T^{3/2}}(T_e - T_i) \Longrightarrow P^H_{ei} = 2P^D_{ei}$$

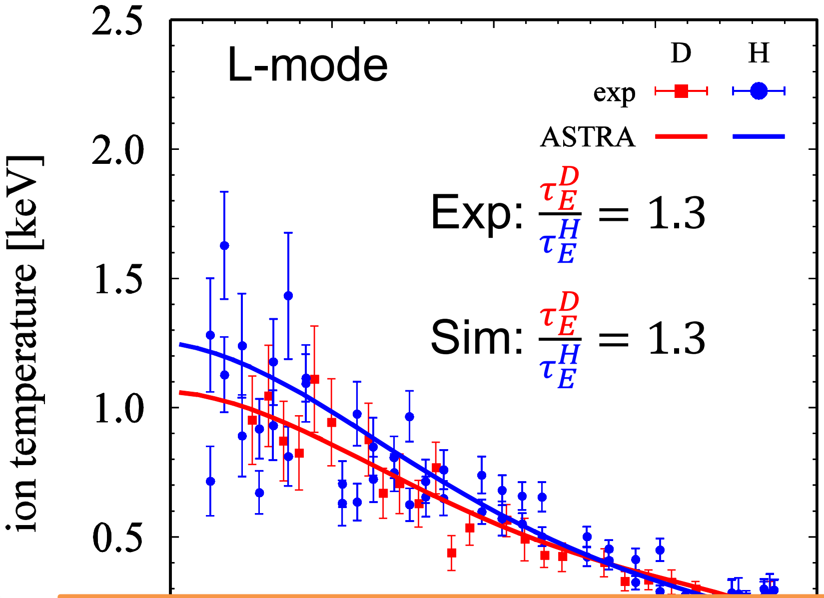

- Confinement effects on He (D, He comparison, He seeding)

  A. Kappatou EX/P8-1 (Fri 14:00)

Heat transport and stiffness of electron and ion channels

F. Ryter EX/P8-3 (Fri 14:00)

First measurements of tilting of density structures

- Eddy tilt angle identified using Doppler-correlation reflectometry.
- Comparison of NBI and ECRH heated plasmas ⟹ change in tilt angle.
  - Measured change in tilt angle mainly from different $E \times B$ flow shear.

PINZON, J. et.al. subm. to PRL

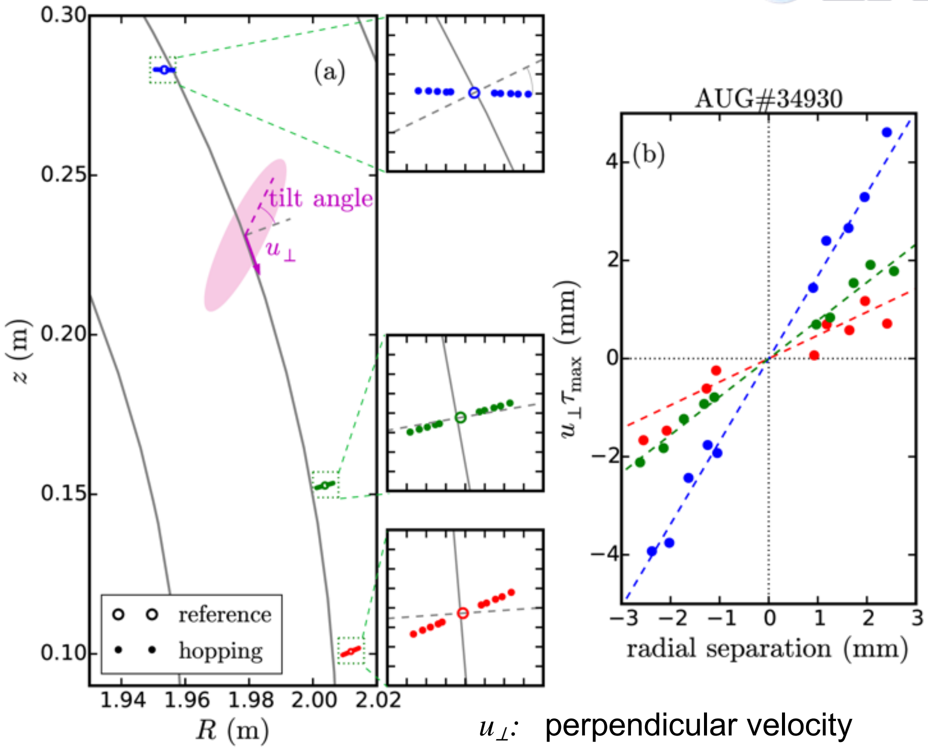

$u_\perp$: perpendicular velocity
τ_{max}: time delay of cross correlation function

Measured $(\tilde{n}_e, \tilde{T}_e)$ phase angle agrees with Gyrokinetics

T. Görler TH/P6-5 (Thu 14:00)

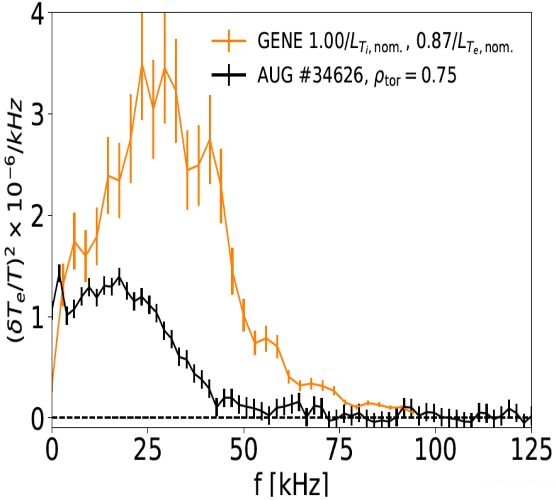

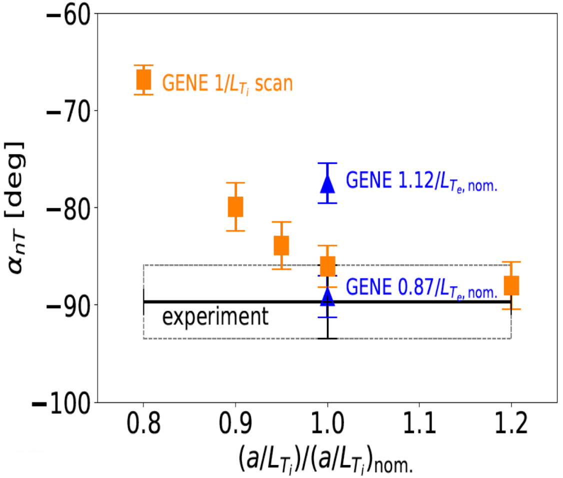

FREETHY, S. J. et al., Physics of Plasmas 25 (2018) 055903.

- Phase angle α_{nT} between $\tilde{n}_e$ and $\tilde{T}_e$ is a **strong constraint for gyro-kinetic simulations**.
- Good agreement with Q_i, Q_e, correlation length $L_r(\tilde{T}_e)$ and α_{nT} with GENE within the experimental uncertainties.
  - Calculated $\tilde{T}_e$ fluctuation spectra tend to be broader and with larger amplitudes then measured.

Gyrokinetics fails to predict convection for light impurities

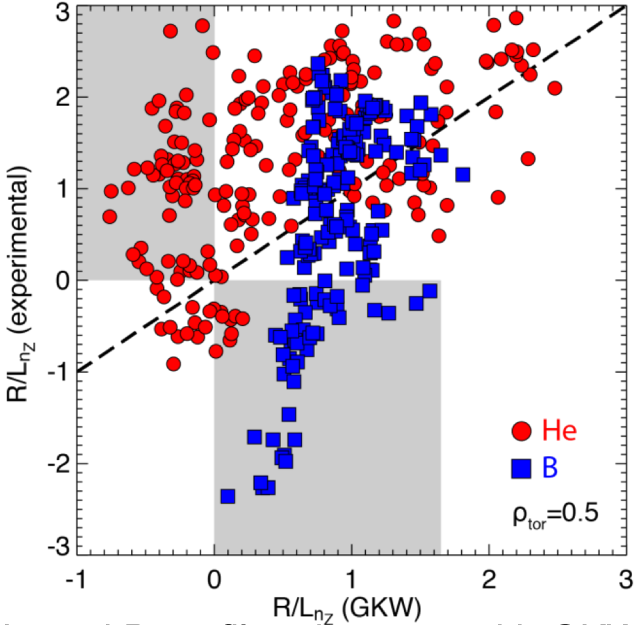

KAPPATOU, A. et al., submitted to Nucl. Fusion.

- Large database: R/L_{n_α} for He and B profiles disagree with GKW.
  - Facilitated by Improved analysis of CXRS[1)] and He plume forward modelling[2)]
    $\Longrightarrow$ accurate impurity density gradients.
- Modulation experiments to determine D and v of B.
- Neocl. + GKW modelling agrees with D, **but predicts v to be in the opposite direction**.

[1)] McDERMOTT, R. . et al., Plasma Phys. Contr. Fusion, 60 (2018) 095007
[2)] KAPPATOU, A. et.al. Plasma Phys. Contr. Fusion, 60 (2018) 055006

Gyrokinetics fails to predict convection for light impurities

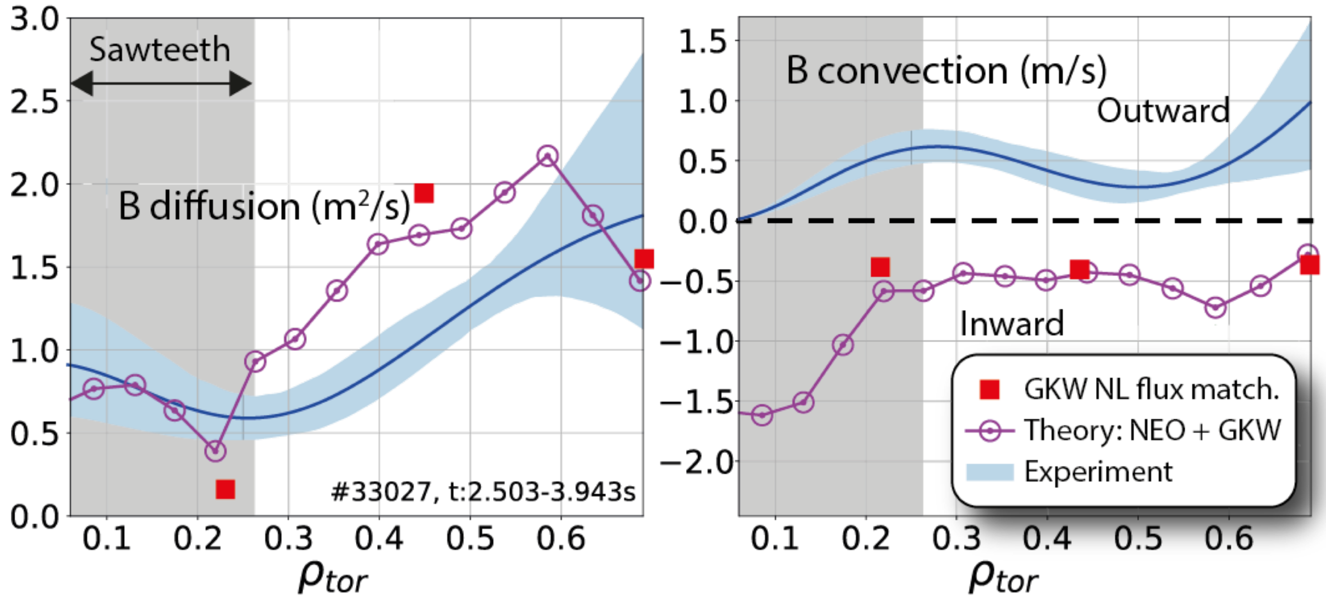

BRUHN, C. et al., Plasma Physics and Controlled Fusion 60 (2018) 085011

Quasi linear GKW:
= linear + saturation

- Large database: R/L_{n_α} for He and B profiles disagree with GKW.
  - Facilitated by Improved analysis of CXRS[1)] and He plume forward modelling[2)] ⟹ accurate impurity density gradients.

KAPPATOU, A. et al., submitted to Nucl. Fusion.

- Modulation experiments to determine D and v of B.

[1)]McDERMOTT, R. . et al., Plasma Phys. Contr. Fusion, 60 (2018) 095007
[2)]KAPPATOU, A. et.al. Plasma Phys. Contr. Fusion, 60 (2018) 055006

- Neocl. + GKW modelling agrees with D, **but predicts v to be in the opposite direction**.

Summary & Outlook

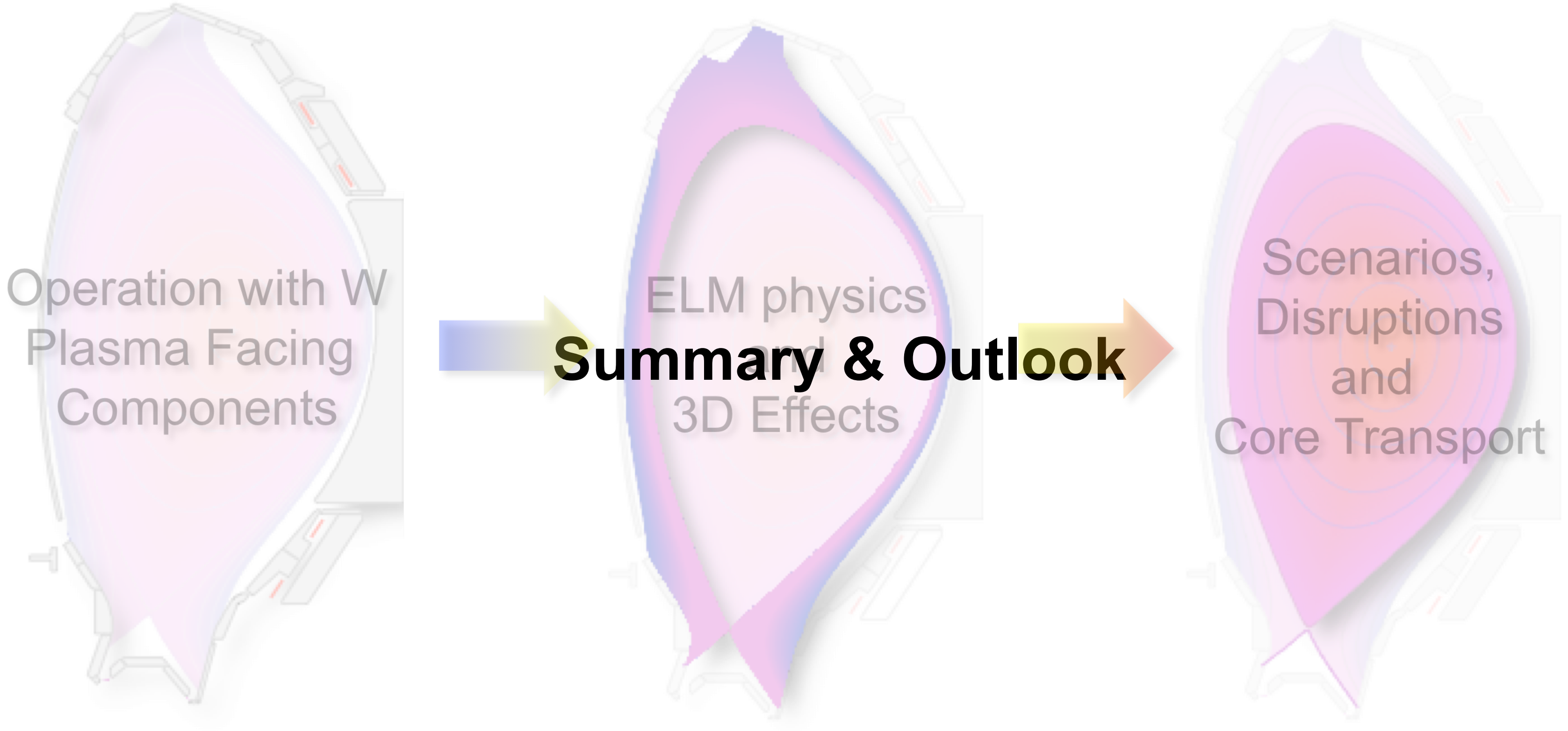

Significant progress in predicting ITER and DEMO

Device

- Upgraded long pulse ECRH (6 MW, 10s)
  - Up to 8 MW by end of 2018.
- New internal coil power supplies.

Edge

- Deep insight into 3D edge physics
  - ELM suppression – achieved with finite $v_{e,\perp}$ over the whole pedestal
  - Helical localised ballooning mode destabilised by bad curvature on field line.
- Reconnection during ELM causes fast ion acceleration.

Core

- New measurements challenge gyro-kinetic modelling
  - Eddy tilt angle measurements consistent with ITG to TEM transition
  - $\tilde{T}_e/T_e$ and (n_e, T_e) phase angle.
- Series of experiment highlight importance of P_{ei} for isotope studies.
  - Important to match electron and ion heating for extrapolation.

The future: New upper divertor to study alternative configurations

HERRMAN, A. et al., SOFT 2018, 16th - 21st Sep., Giardini Naxos, Italy, 2018.

Hardware:

- Two new in-vessel coils
- Cryogenic pump
- Better diagnostics

Studies:

- Alternative configurations at high heat flux
  - X-divertor.
  - Snow-Flake divertor.
  - Flux expansion.
- Two fluid simulations (SOLPS) predict strong reduction in heat-flux

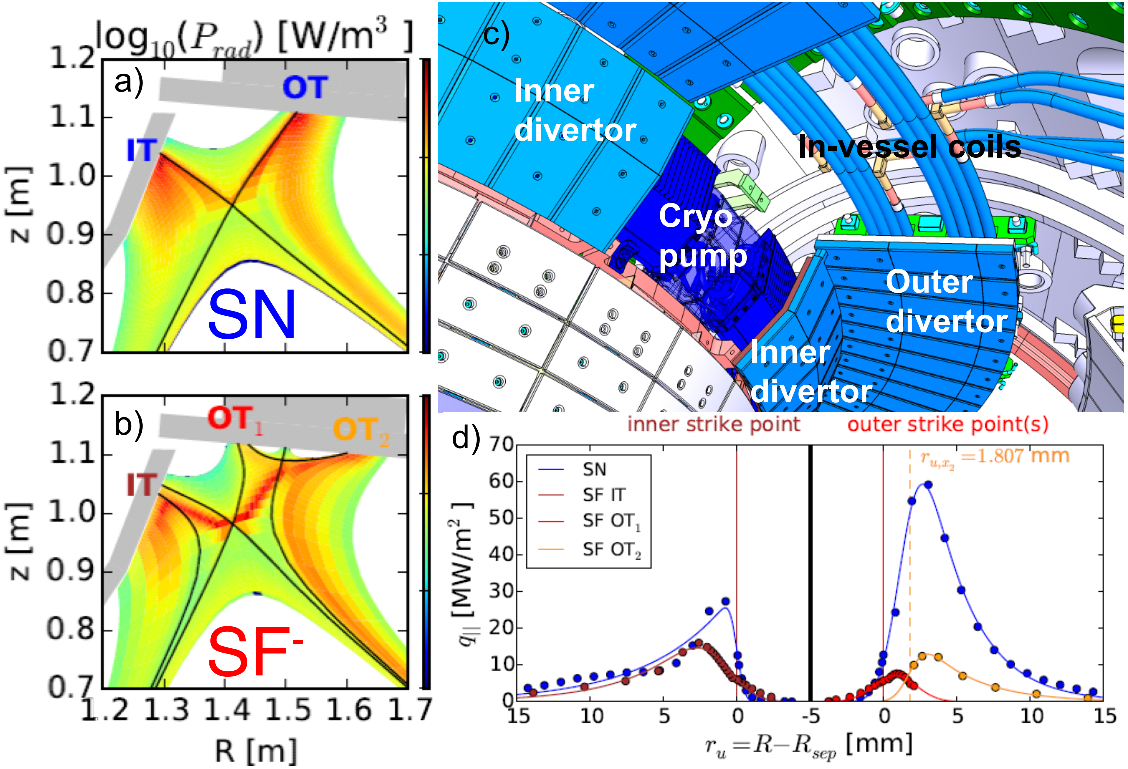

PAN, O. et al., Plasma Physics and Controlled Fusion 60 (2018) 085005

The future: New upper divertor to study alternative configurations

Hardwar

- Two n
- Cryog
- Better

Studies:

- Alterna at high
  - X-d
  - Sno
  - Flux
- Two fl (SOLP reduct

SOFT 2018, 16th - axos, Italy, 2018.

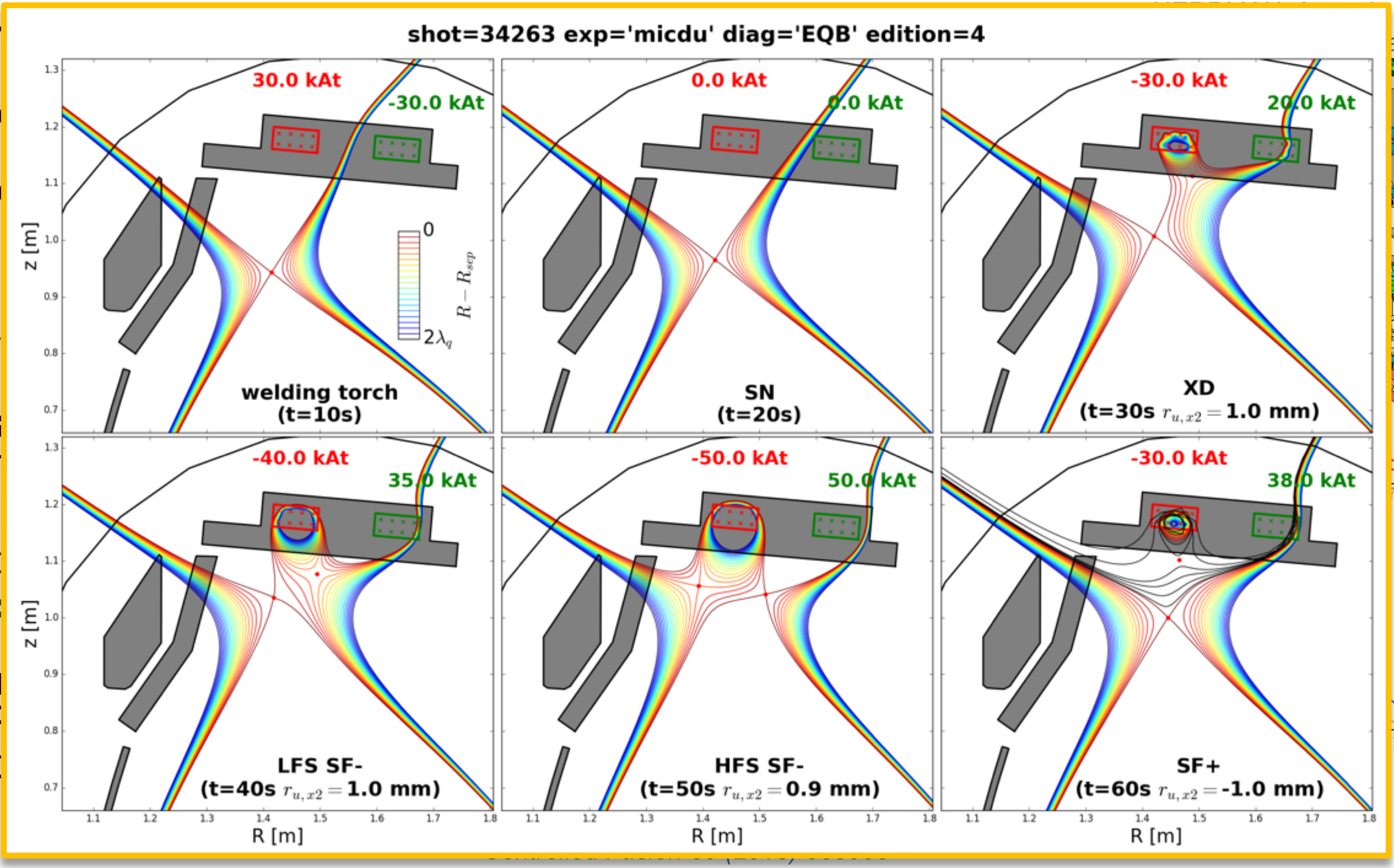

AUG related contributions at this conference

Pedestal & ELMs

- ***S.J.P. Pamela*** OV/4-4 (Tue 15:25) - oral
- ***B. Labit*** EX/2-5 (Wed 12:05) – oral
- ***W. Suttrop*** EX/7-3 (Fri 9:10) - oral
- ***F. Laggner*** EX/P6-4 (Thu 14:00)
- ***M. Dunne*** EX/P8-2 (Fri 14:00)
- ***E. Viezzer*** EX/P8-5 (Fri 14:00)
- ***C. Silva*** EX/P8-11 (Fri 14:00)

SOL & Divertor

- ***R. Lunsford*** FIP/2-3 (Thu 15:00) - oral
- ***A.H. Nielsen*** TH/P7-4 (Fri 8:30)
- ***M. Wischmeier*** TH/P7-5 (Fri 8:30)
- ***N. Vianello*** EX/P8-13 (Fri 14:00)

Scenario & Heating:

- ***T. Happel*** EX/2-3 (Wed 11:25) - oral
- ***Y. Kazakov*** EX/8-1 (Fri 15:20) - oral
- ***T. Pütterich*** EX/P8-4 (Fri 14:00)
- ***L. Frassinetti*** EX/P8-22 (Fri 14:00)
- ***J.M. Noterdaeme*** EX/P8-23 (Fri 14:00)

Transport & Confinement:

- ***F. Ryter*** EX/P8-3 (Fri 14:00)
- ***T. Görler*** TH/P6-5 (Thu 14:00)
- ***G. Verdoolage*** EX/P7-1 (Fri 8:30)
- ***A. Kappatou*** EX/P8-1 (Fri 14:00)

MHD:

- ***E. Strait*** OV/4-5 (Tue 15:40) – oral
- ***F. Lui*** TH/P5-18 (Thu 8:30)
- ***A. Snicker*** TH/P2-8 (Tue 14:00)
- ***M. Willensdorfer*** EX/P8-20 (Fri 14:00)
- ***V. Igochine*** EX/P8-21 (Fri 14:00)

Fast Ions & Current Drive

- ***P. Lauber*** EX/1-1 (Tue 10:45) – oral
- ***M. Weiland*** TH/6-3 (Fri 14:00) - oral
- ***B. Geiger*** EX/P8-24 (Fri 14:00)
- ***D. Rittich*** EX/P8-25 (Fri 14:00)
- ***J. Galdon-Quiroga*** EX/P8-26 (Fri 14:00)

Thanks to all the contributors

ASDEX Upgrade

Austrian Academy of Sciences
AUSTRIA

Ecole Royale Militaire Laboratory for Plasma Physics
BELGIUM

Bulgarian Academy of Sciences
BULGARIA

Ruđer Bošković Institute
CROATIA

University of Cyprus
CYPRUS

Institute of Plasma Physics Academy of Sciences of the Czech Republic
CZECH REPUBLIC

Technical University of Denmark
DENMARK

University of Tartu
ESTONIA

Technical Research Centre of Finland
FINLAND

atomique et aux énergies alternatives
FRANCE

JÜLICH FORSCHUNGSZENTRUM
GERMANY

Karlsruhe Institute of Technology
GERMANY

Max-Planck-Institut für Plasmaphysik
GERMANY

National Center for Scientific Research "Demokritos"
GREECE

Wigner Research Centre for Physics
HUNGARY

Dublin City University
IRELAND

Agenzia nazionale per le nuove tecnologie, l'energia e lo sviluppo economico sostenibile
ITALY

LATVIJAS UNIVERSITĀTE
LATVIA

Lithuanian Energy Institute
LITHUANIA

Institute of Plasma Physics and Laser Microfusion
POLAND

Instituto Superior Técnico
PORTUGAL

Institute for Atomic Physics
ROMANIA

Comenius University
SLOVAKIA

Jožef Stefan Institute
SLOVENIA

Centro de Investigaciones Energéticas Medioambientales y Tecnológicas
SPAIN

Swedish Research Council
SWEDEN

École polytechnique fédérale de Lausanne
SWITZERLAND

Foundation for Fundamental Research on Matter
THE NETHERLANDS

CCFE CULHAM CENTRE FOR FUSION ENERGY
UNITED KINGDOM

Princeton Plasma Physics Laboratory
United States

Massachusetts Institute of Technology
United States

General Atomics
United States